

Ocean Diurnal Variations Measured by the Korean Geostationary Ocean Color Imager

Menghua Wang¹, Lide Jiang^{1,2}, Seunghyun Son^{1,2}, & Wei Shi^{1,2}

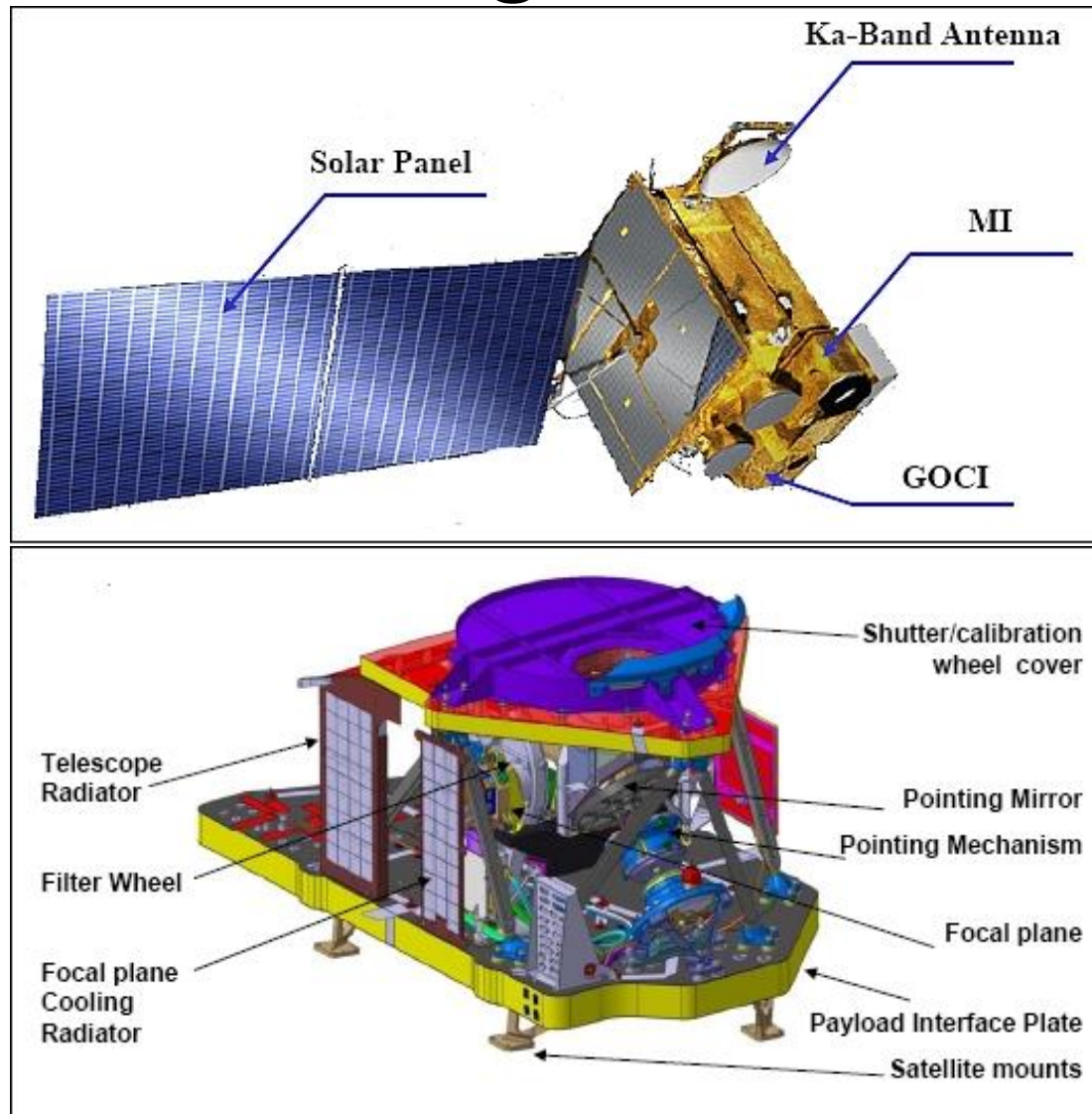
¹ NOAA/NESDIS Center for Satellite Applications & Research (STAR)
College Park, MD, USA

² CIRA, Colorado State University, Fort Collins, CO, USA

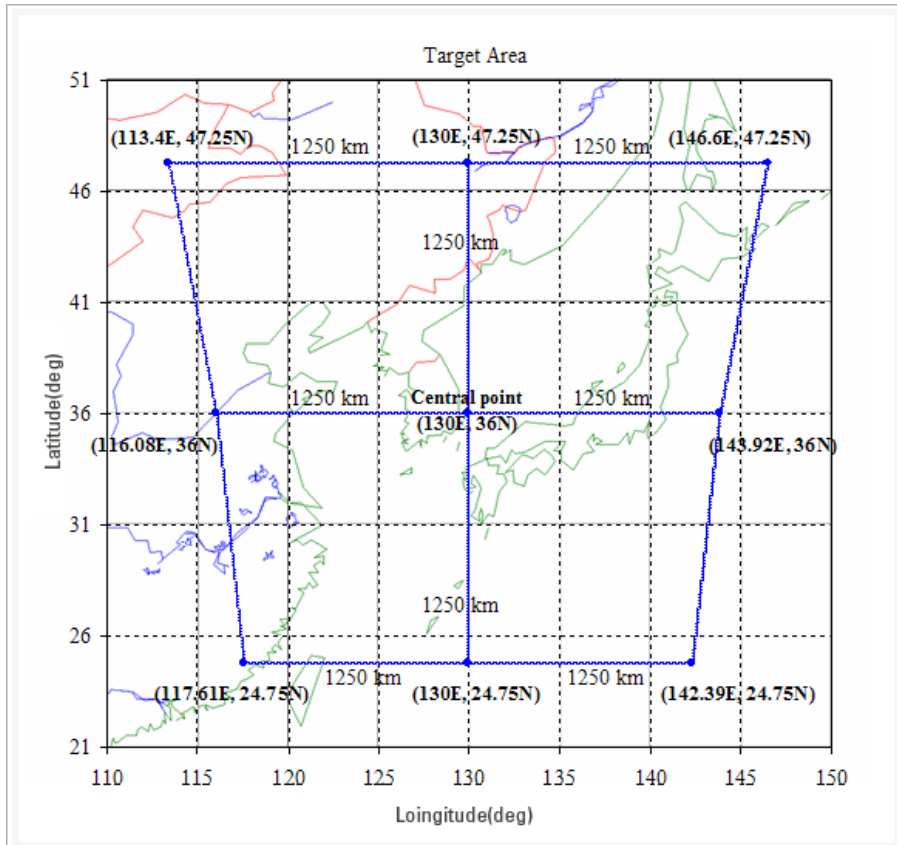
July 24th, 2013

at ‘CoRP 9th Annual Science Symposium’ in Madison, Wisconsin

COMS-1 – Communication, Ocean and Meteorological Satellite



GOCl Introduction



- 412nm Yellow substance and turbidity
- 443nm Chlorophyll absorption maximum
- 490nm Chlorophyll and other pigments
- 555nm Turbidity, suspended sediment
- 660nm Baseline of fluorescence signal,
Chlorophyll, suspended sediment
- 680nm Atmospheric correction and fluorescence
signal
- 745nm Atmospheric correction and baseline of
fluorescence signal
- 865nm Aerosol optical thickness, vegetation,
water vapor reference over the ocean

NOAA-MSL12 Processing for GOCI data

- Collaboration effort between NOAA/NESDIS/STAR and KIOST/KOSC.
- NOAA-MSL12 data processing (based on NASA SeaDAS) is improved for the GOCI data processing.
- Various parameters and **lookup tables** are generated, and a **new atmospheric correction algorithm** has been developed for GOCI data processing in the region (Wang *et al.*, 2012; 2013).
- **New cloud masking method** has been recently developed for very turbid coastal waters (e.g., Yangtze River mouth, Korean Coastal areas).
- The GOCI atmospheric correction algorithm is recently improved using **new vicarious calibration**.
- GOCI Level-1B data (Mar. 2011– Feb. 2013) were obtained from the Korea Ocean Satellite Center and processed using the new atmospheric correction algorithm.
- In situ optical measurements (Mar.– Nov. 2011) are used to quantify and validate GOCI ocean color products with the new atmospheric correction algorithm for GOCI ocean color data processing.

Estimating NIR Contribution

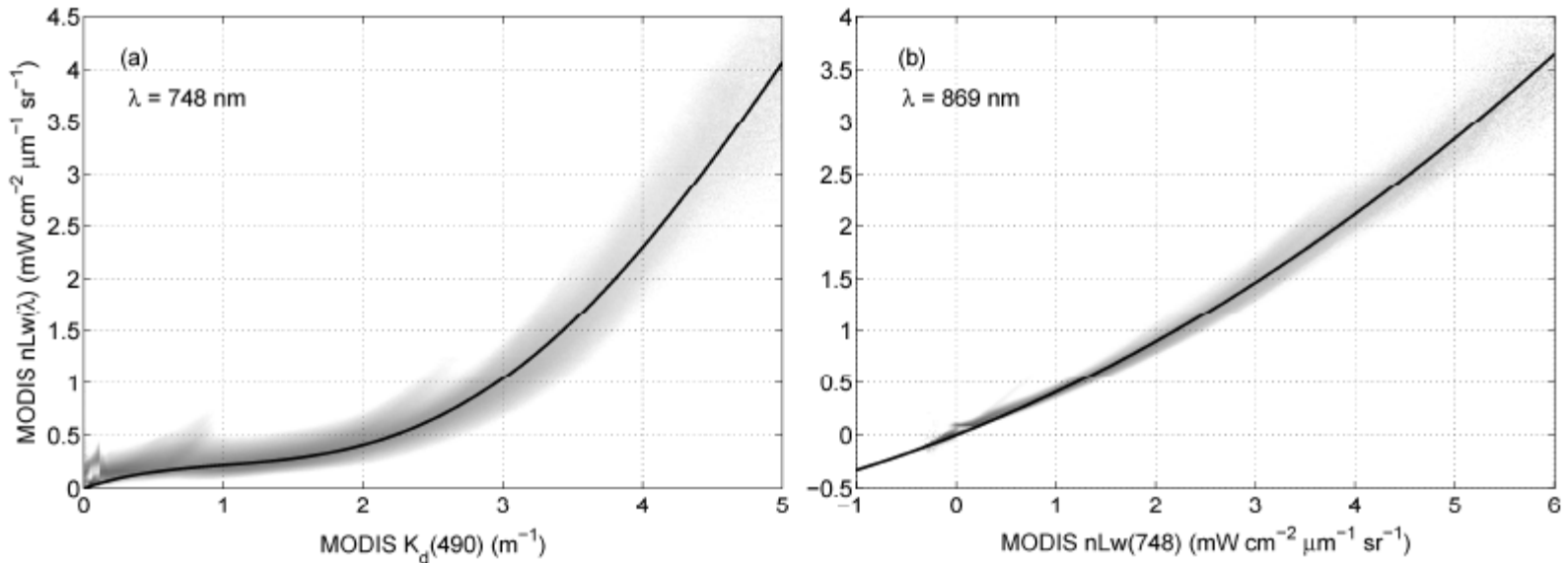
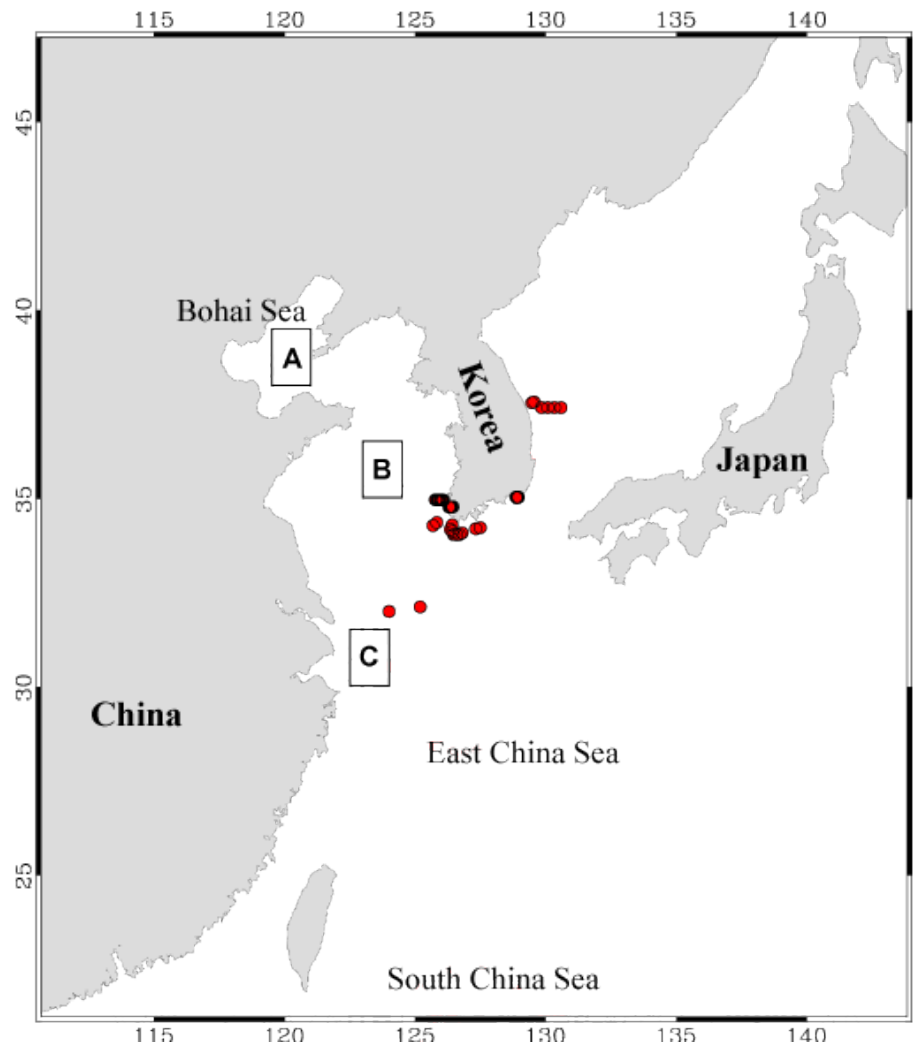


Fig. 2. Scatter plots and empirical polynomial fitting functions for (a) $nL_w(748)$ vs. $K_d(490)$ and (b) $nL_w(869)$ vs. $nL_w(748)$. Note that $nL_w(748)$, $nL_w(869)$, and $K_d(490)$ were derived from MODIS-Aqua measurements (2002 to 2009) using the SWIR atmospheric correction algorithm in this region.

- $nLw(748) = f(Kd(490))$, $f(x) = 0.465x - 0.385x^2 + 0.152x^3 - 0.0121x^4$
- $nLw(869) = g(nLw(748))$, $g(x) = 0.368x + 0.04x^2$
- *M. Wang, W. Shi, and L. Jiang, "Atmospheric correction using near-infrared bands for satellite ocean color data processing in the turbid western Pacific region", Optical Express, 20(2), 741-753 (2012)*

GOCI Coverage over Korean Peninsular and location of in-situ measurements

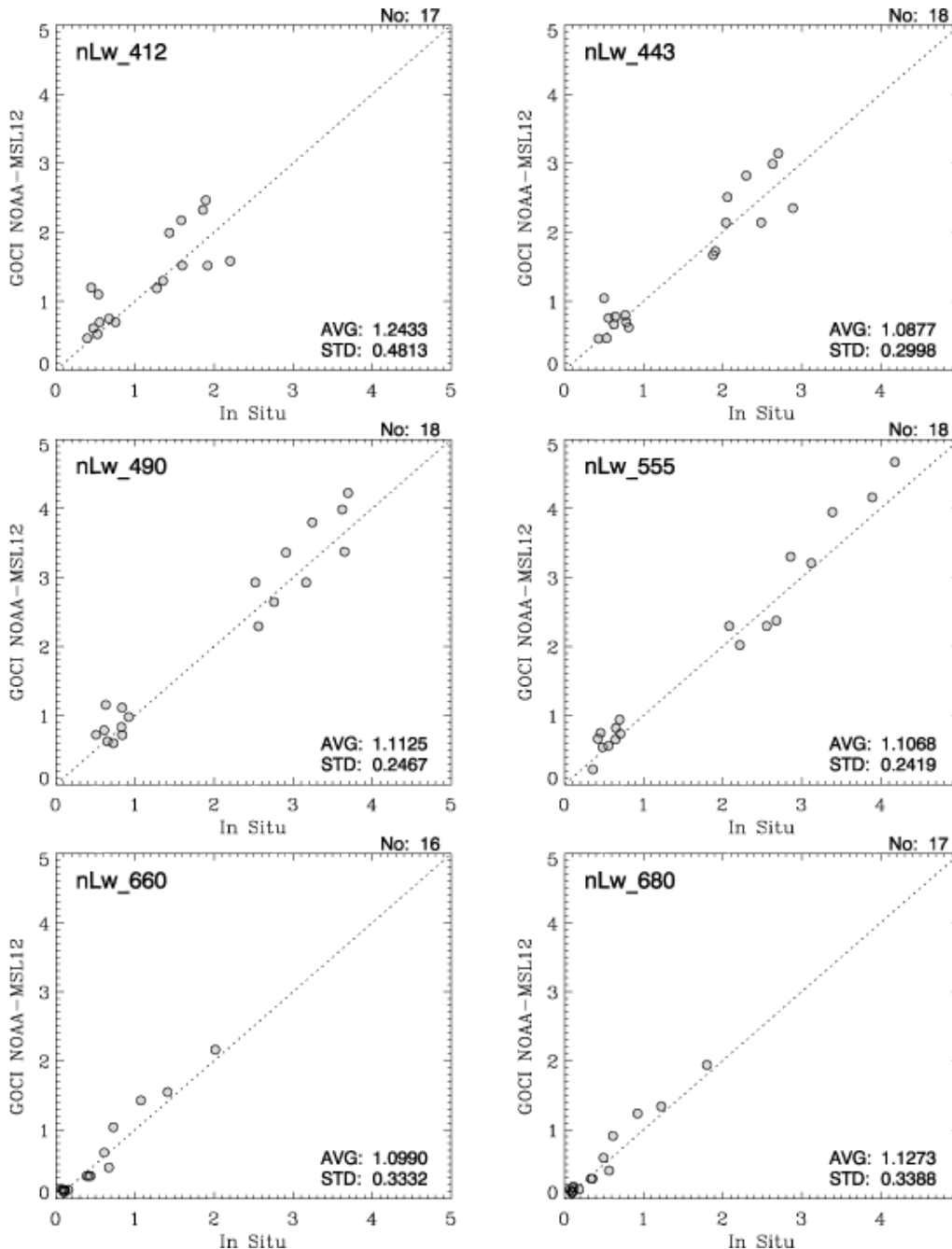


*. In-situ bio-optical measurements are provided by KIOST/KOSC

GOCI Matchup Comparison

M. Wang, J.H. Ahn, L. Jiang, W. Shi, S. Son, Y.J. Park, and J.H. Ryu, “Ocean color products from the Korean Geostationary Ocean Color Imager (GOCI)”, Optical Express, 21(3), 3835-3849 (2013)

Matchup between **in-situ** and **GOCI NOAA-MSL12** using **New Gain**

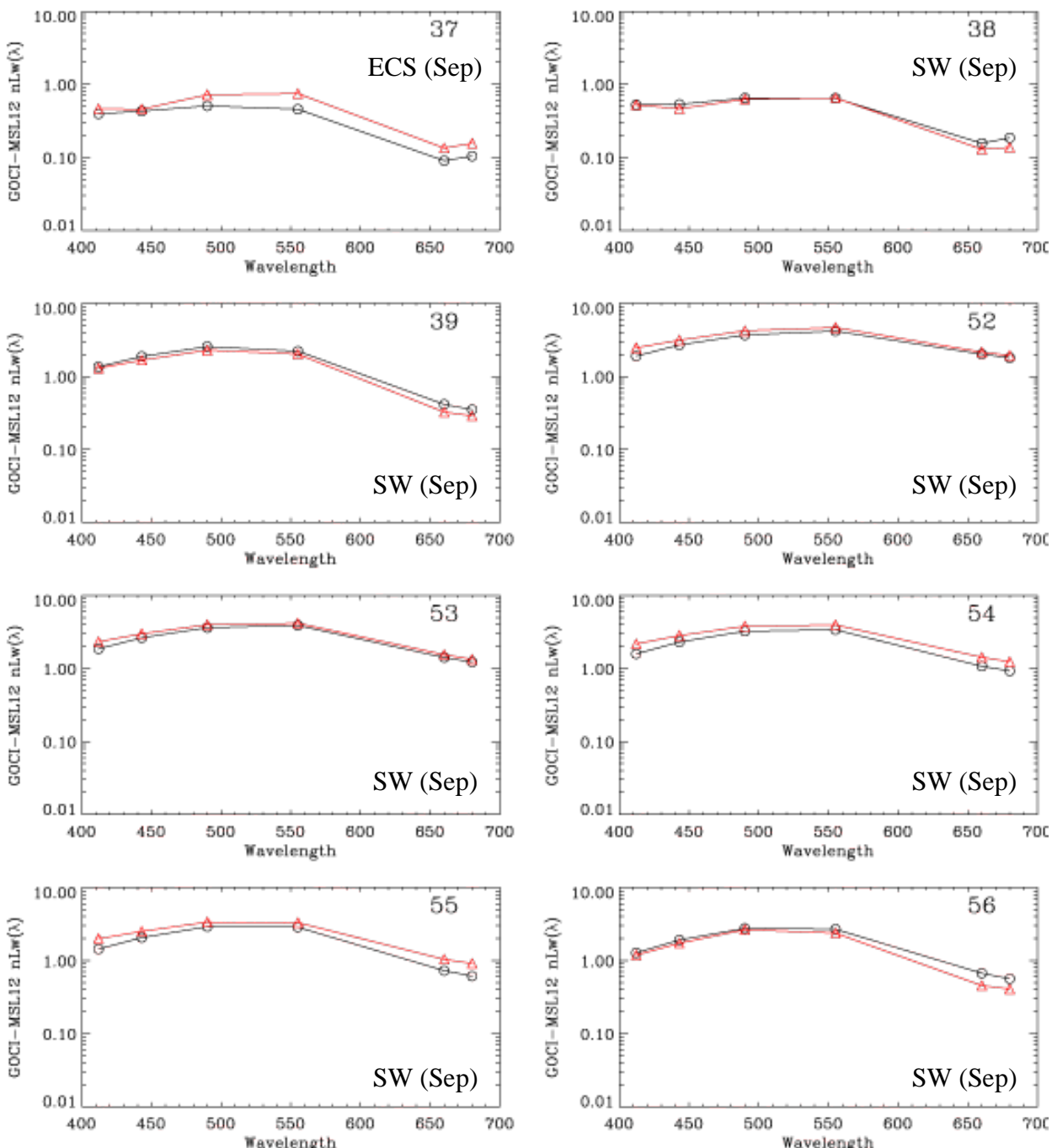


Mean Ratio of GOCI NOAA-MSL12 vs. In Situ

Var	Old (Wang et al. 2013)		New Gain	
	Avg (std)	No	Avg (std)	No
$nL_w(413)$	1.2737 (0.599)	18	1.2433 (0.481)	17
$nL_w(443)$	1.4182 (0.486)	18	1.0677 (0.300)	18
$nL_w(490)$	1.2868 (0.357)	18	1.1125 (0.247)	18
$nL_w(555)$	1.1506 (0.308)	18	1.1068 (0.242)	18
$nL_w(660)$	1.3367 (0.531)	18	1.0990 (0.333)	16
$nL_w(680)$	1.4092 (0.586)	17	1.1273 (0.339)	17

Black-in situ, red-GOCI

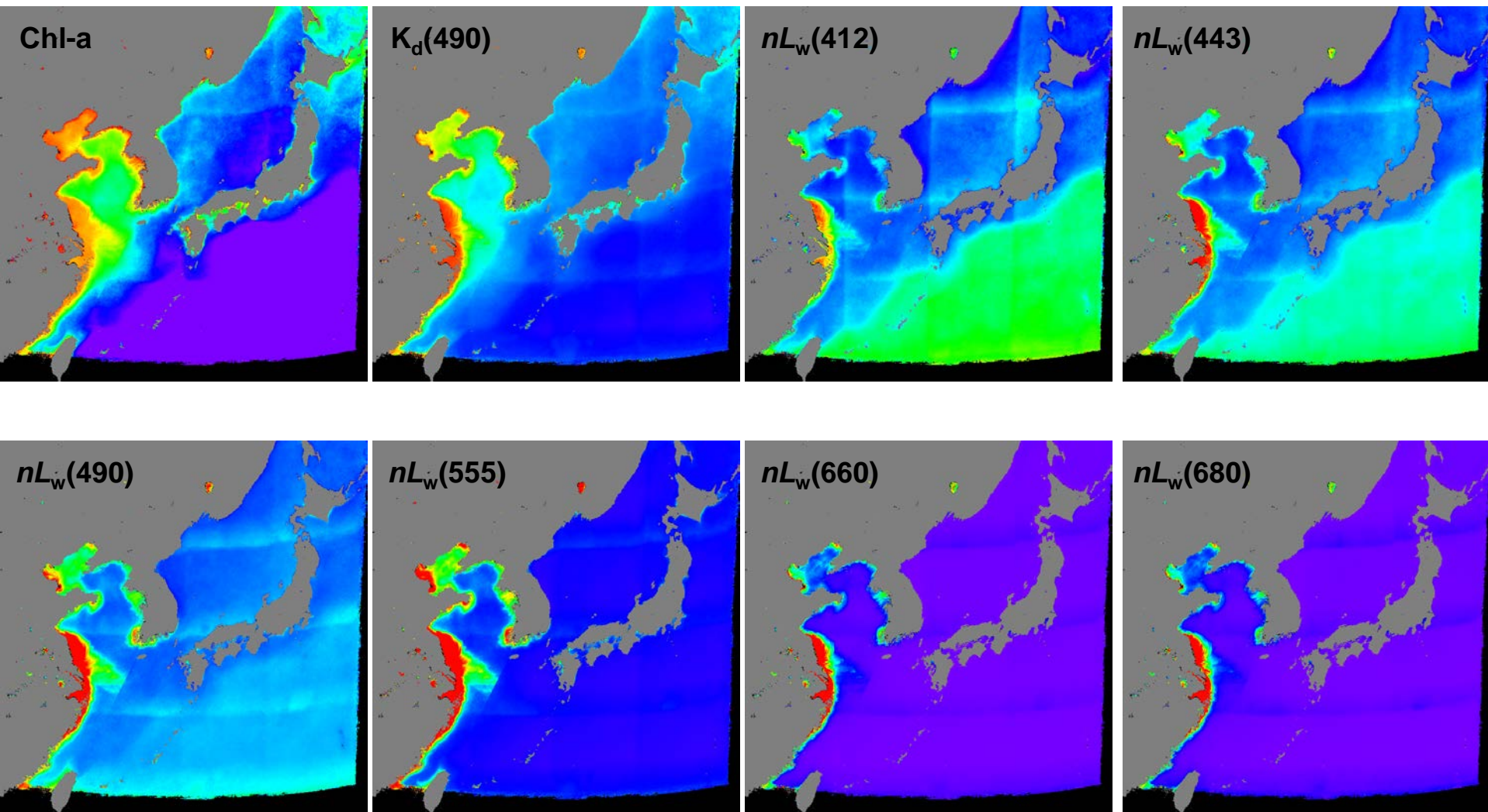
Spectral shape of *in situ* and GOCI-derived $nL_w(\lambda)$ measurements



GOCI Composite Images

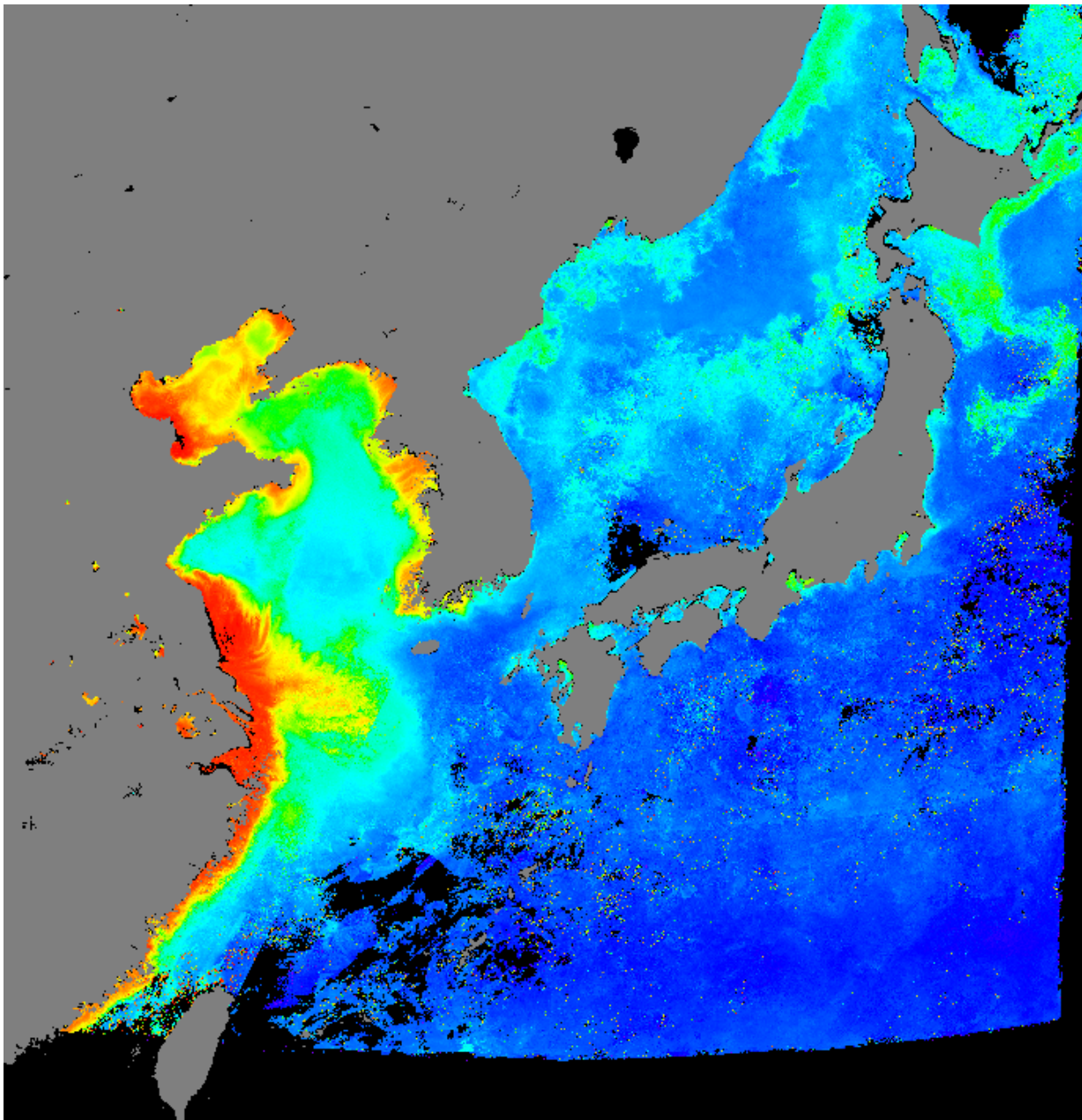
(2011 Mar. – 2012 Oct.)

Climatology GOCl Images from Mar. 2011 to Oct. 2012 (at 12:00)

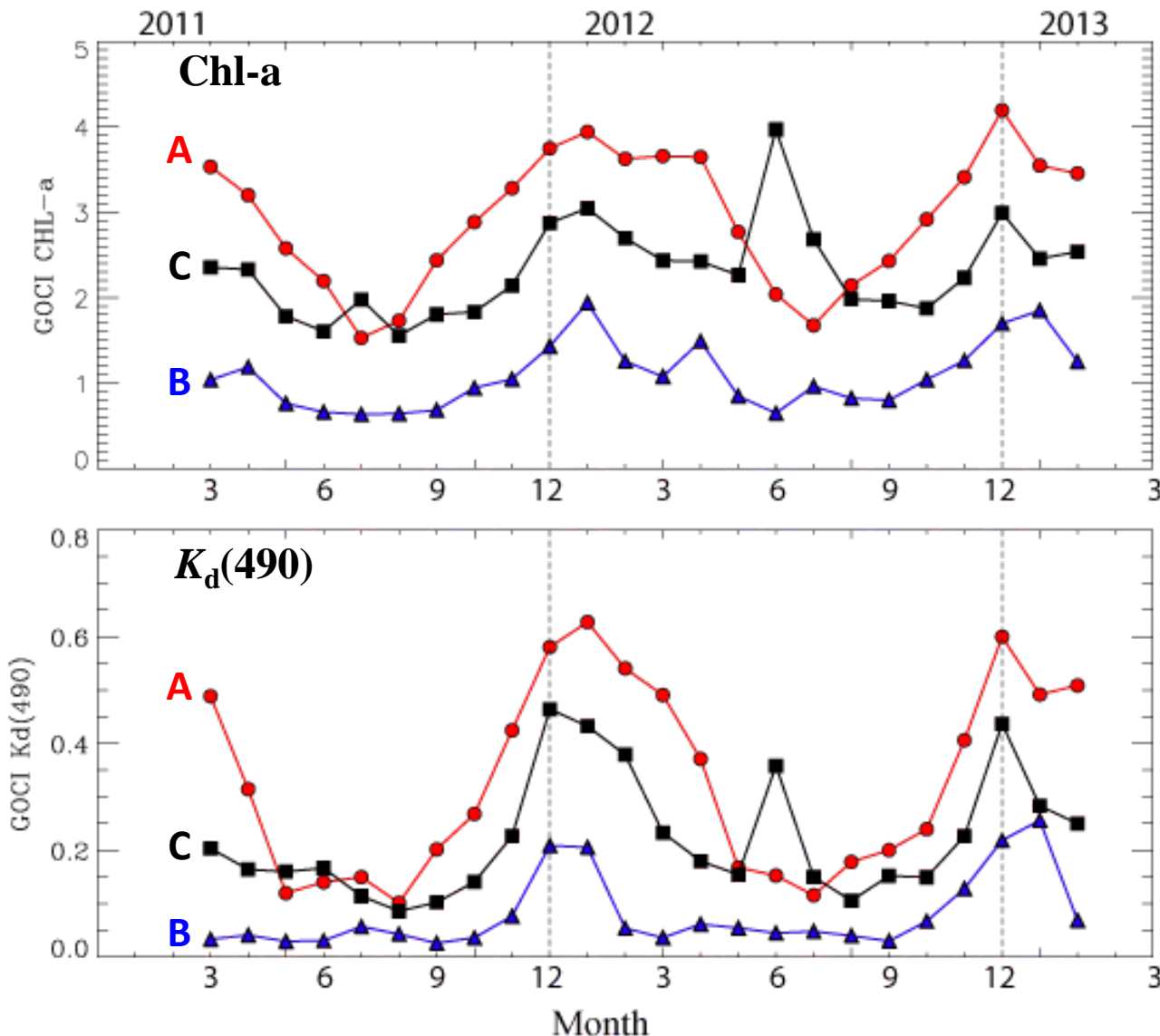


Monthly Composite Images of GOCI $K_d(490)$

(Mar. 2011 – Oct. 2012, at 12:00)

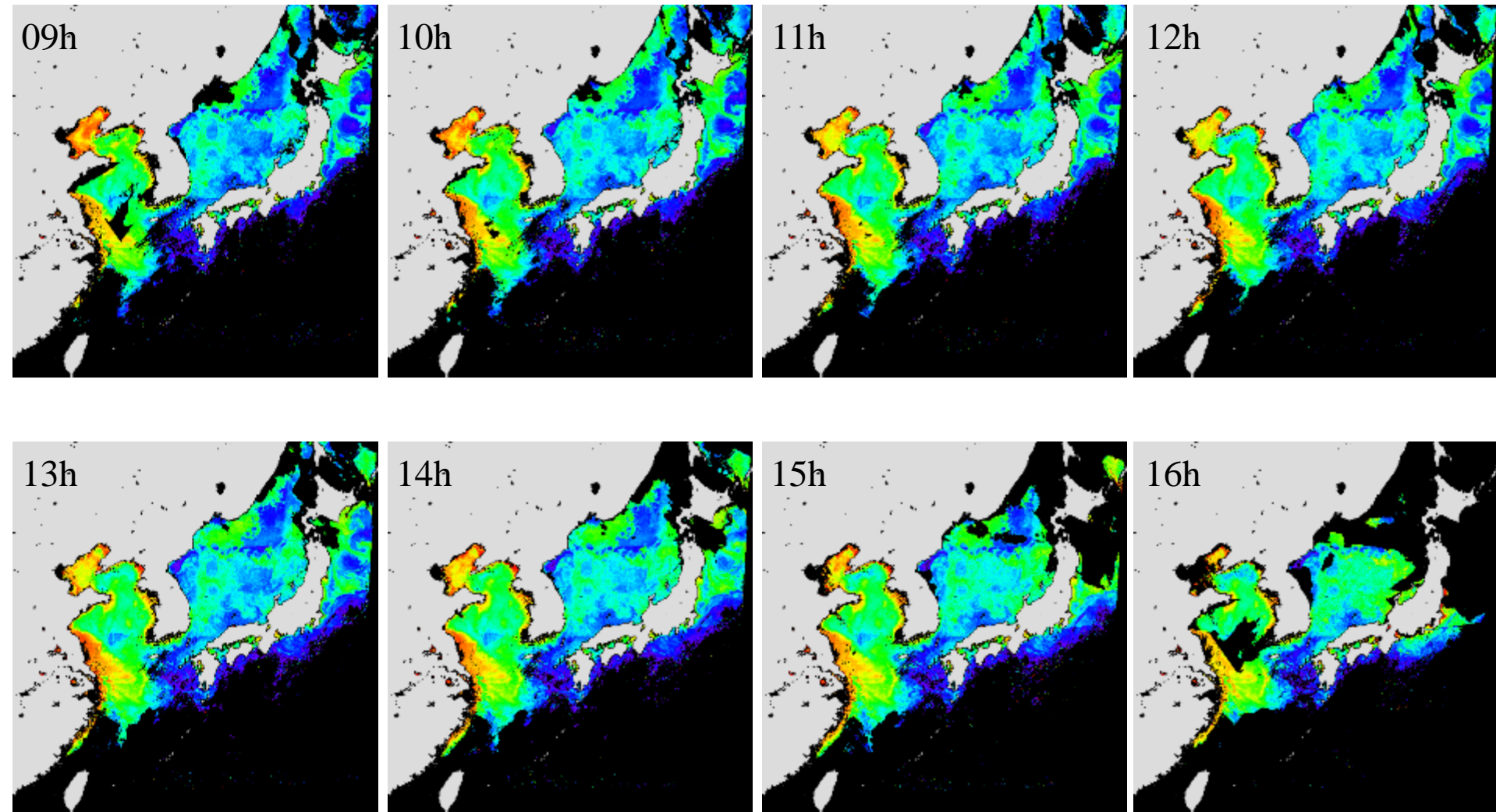


Time Series of GOCI *Chl-a* & *K_d(490)* Monthly Mean (Mar. 2011 – Oct. 2012, at 12:00)



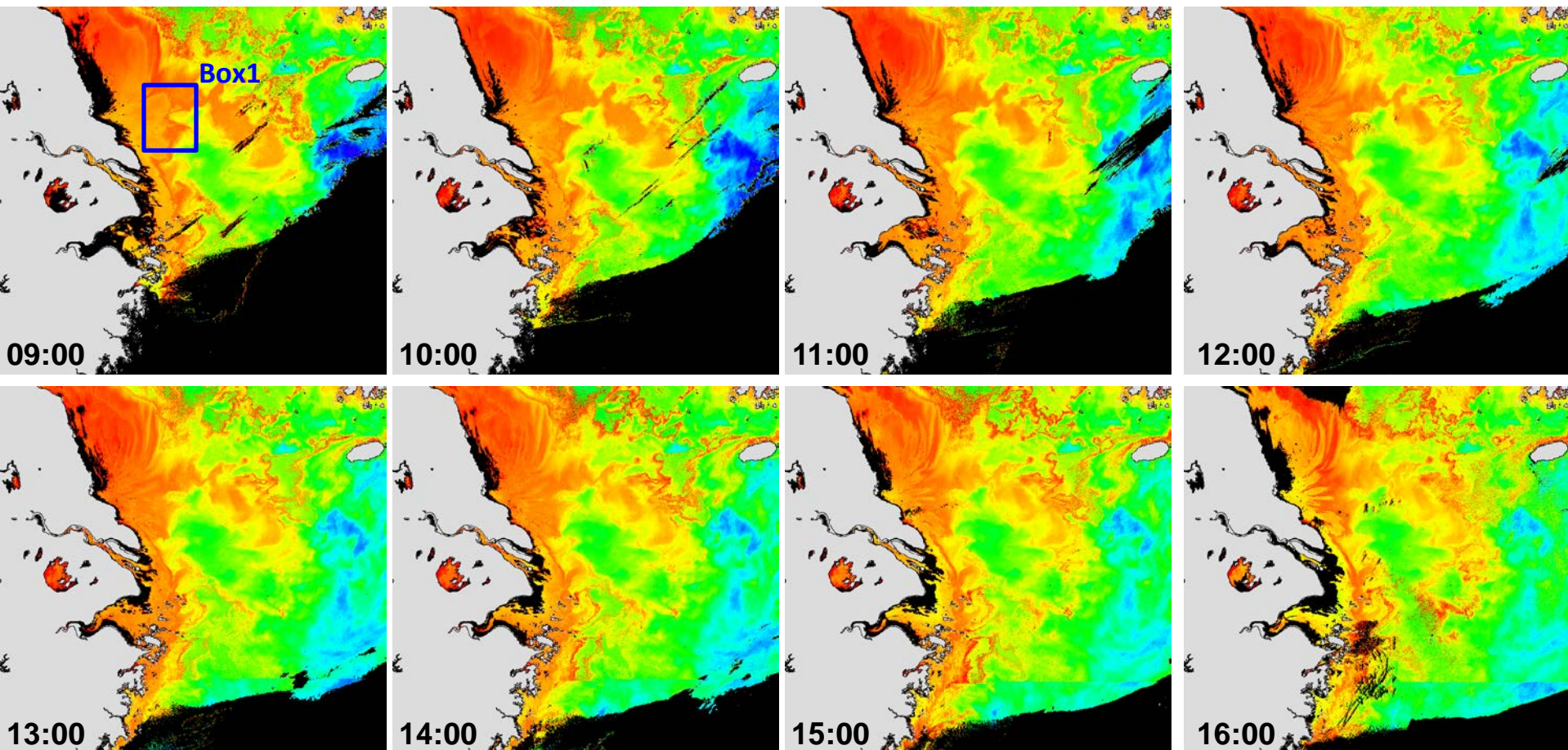
GOCI Images for Diurnal Changes

GOCI-MSL12 Chl-a (Apr. 5, 2011)

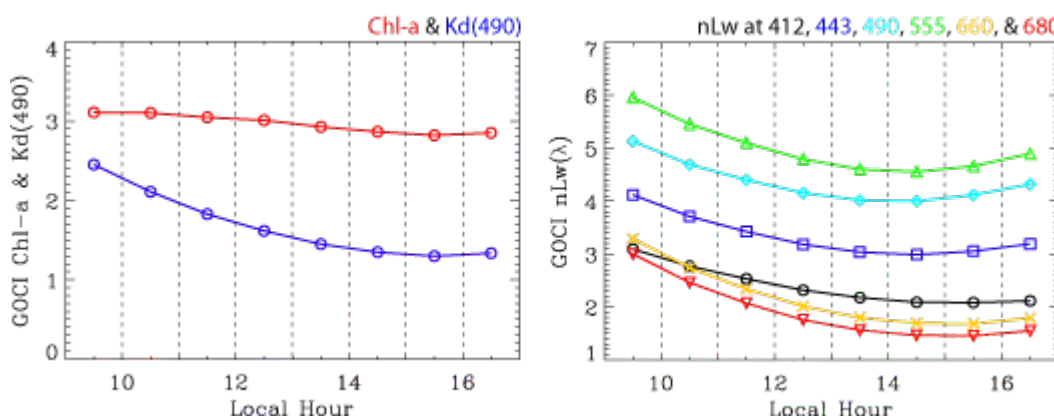


GOCI Images in the East China Sea

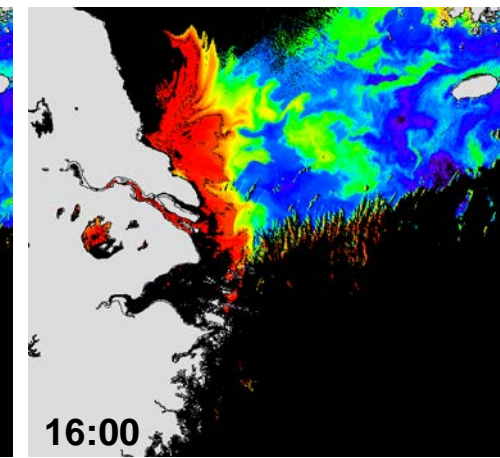
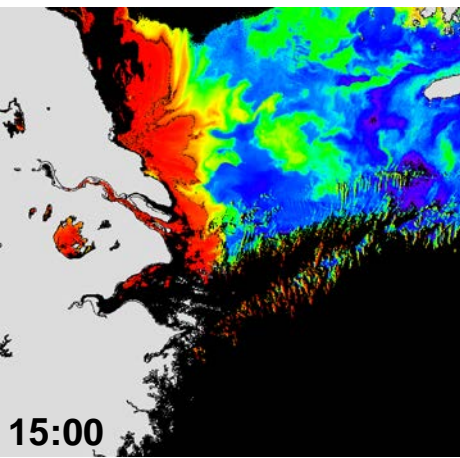
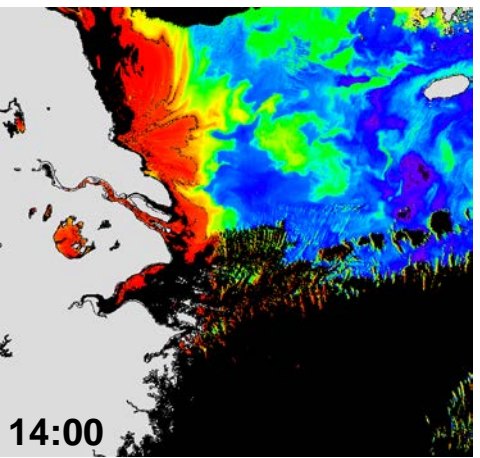
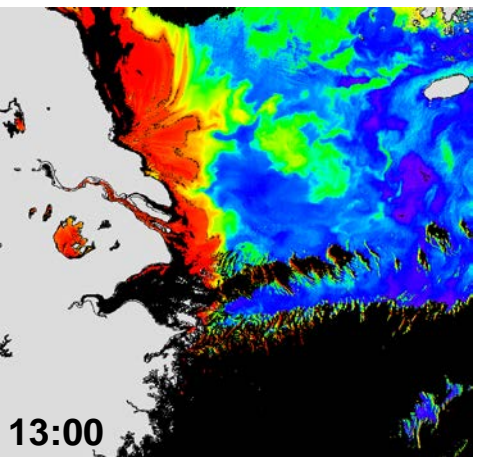
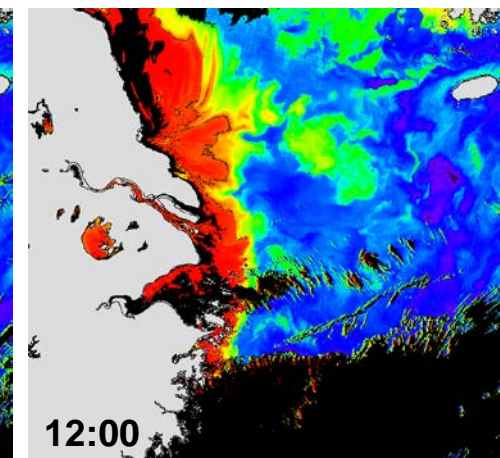
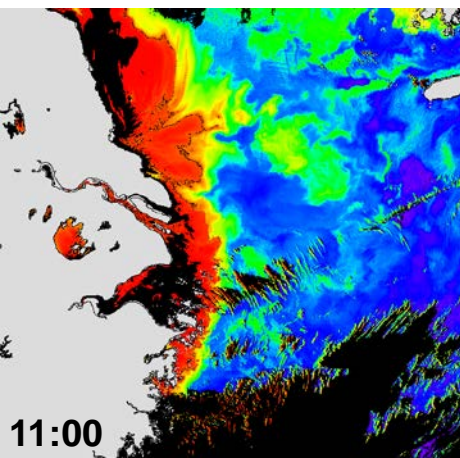
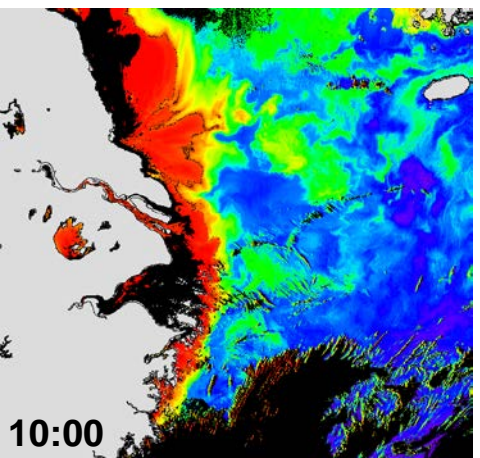
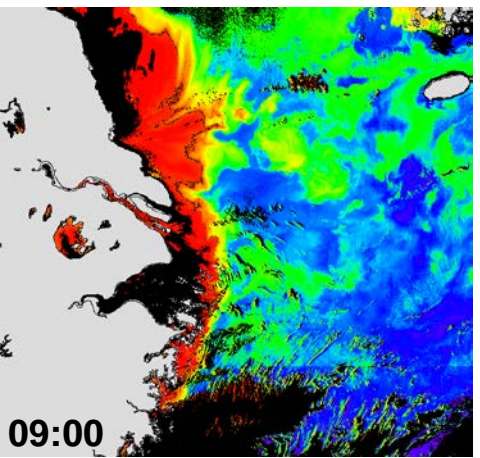
GOCI NOAA-MSL12 Chl-a (2012-04-26)



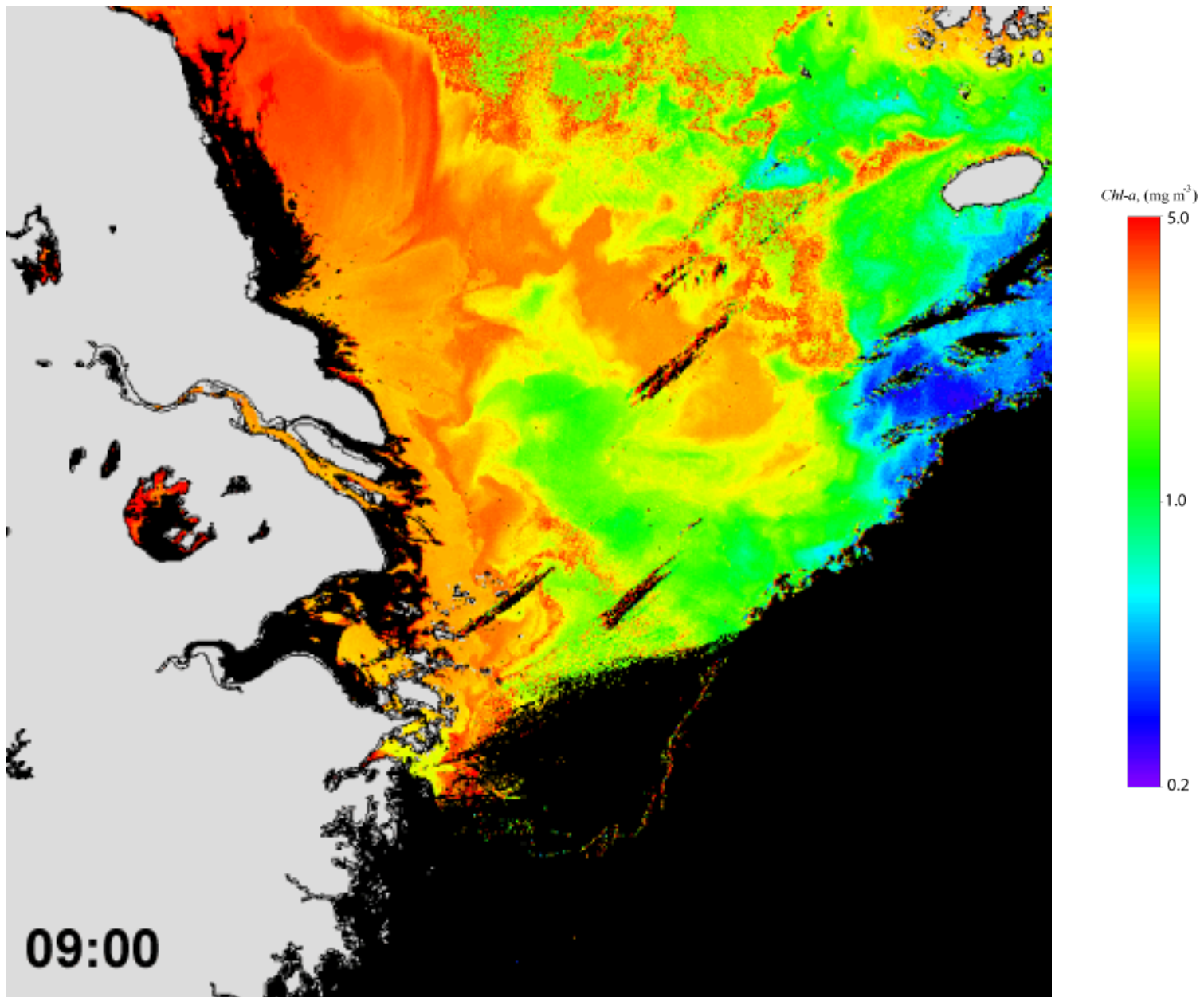
Diurnal Changes



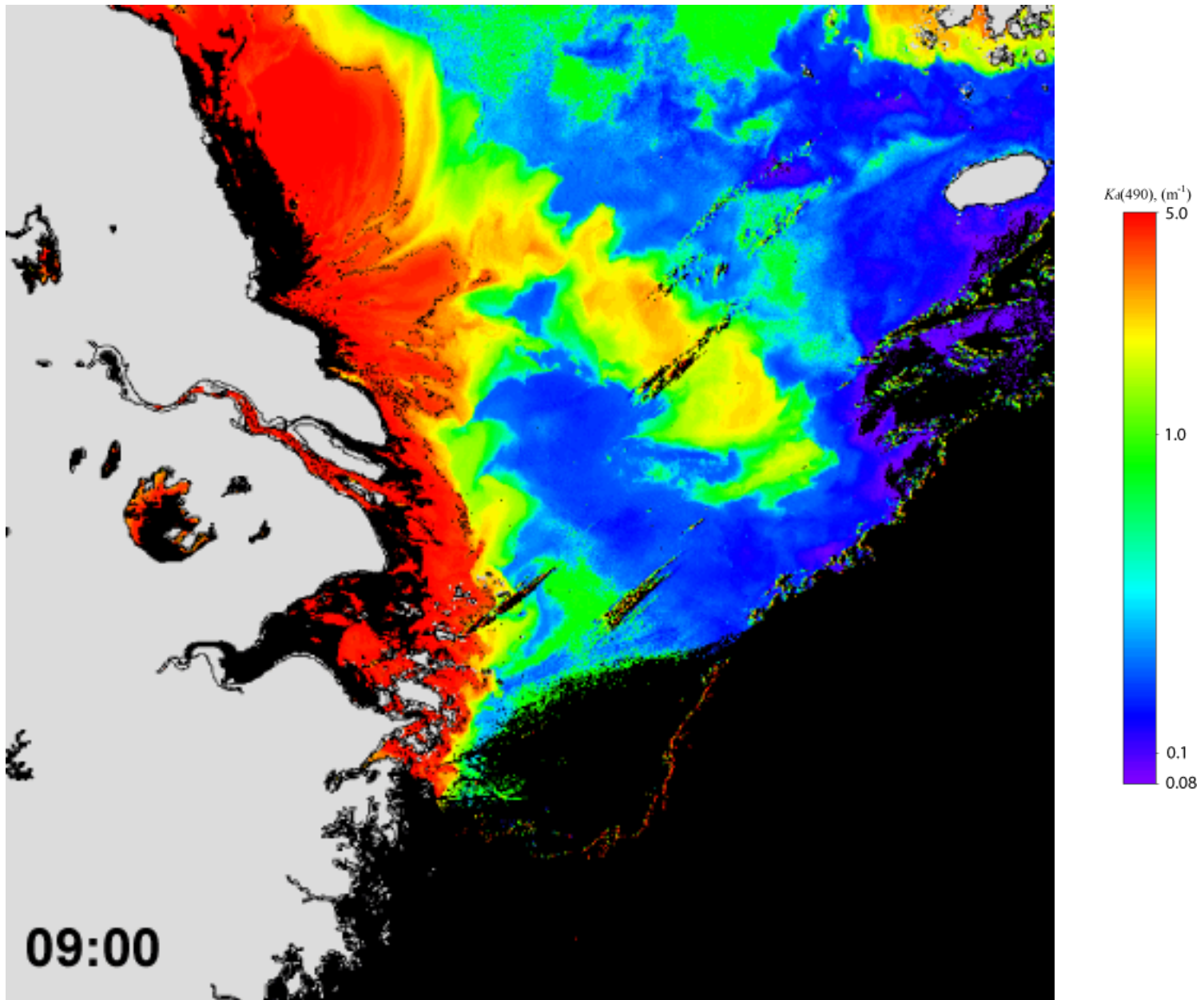
GOCI NOAA-MSL12 $K_d(490)$ (2012-04-27)



GOCI NOAA-MSL12 Chl-a (2012-04-26)

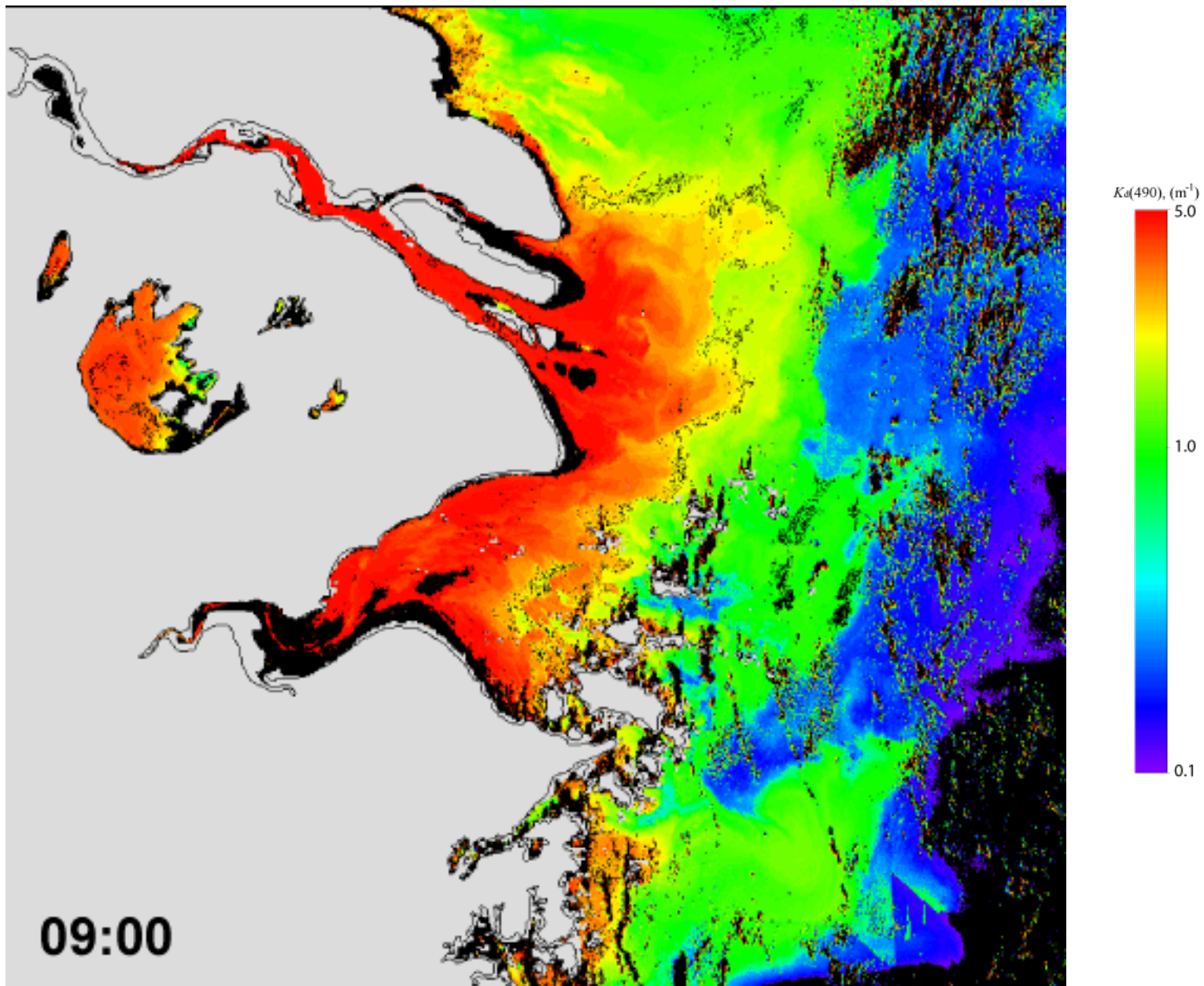


GOCI NOAA-MSL12 $K_d(490)$ (2012-04-26)



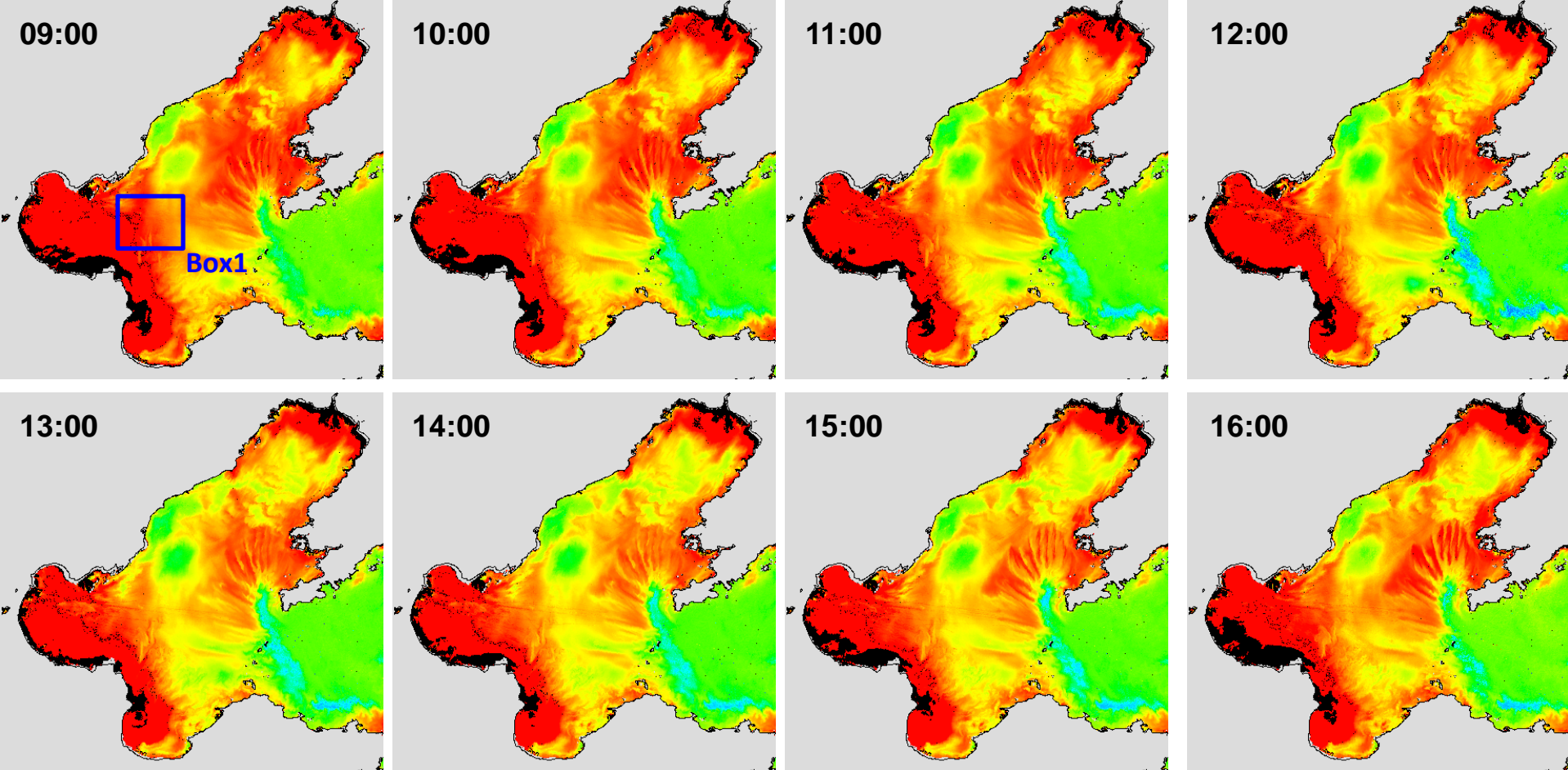
**GOCI Images in
Hangzhou Bay & Lake Taihu**

GOCI NOAA-MSL12 $K_d(490)$ (2012-07-29)

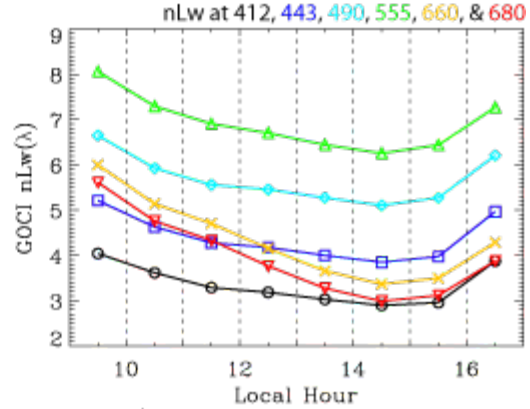
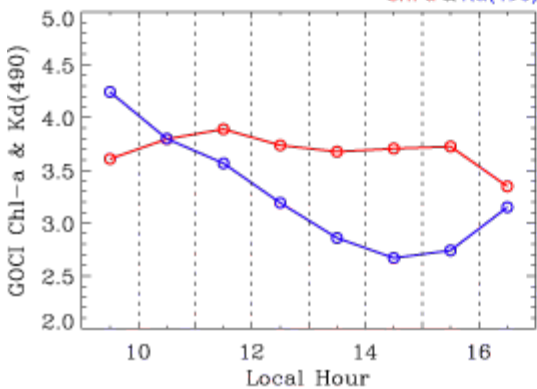


GOCI Images in the Bohai Sea

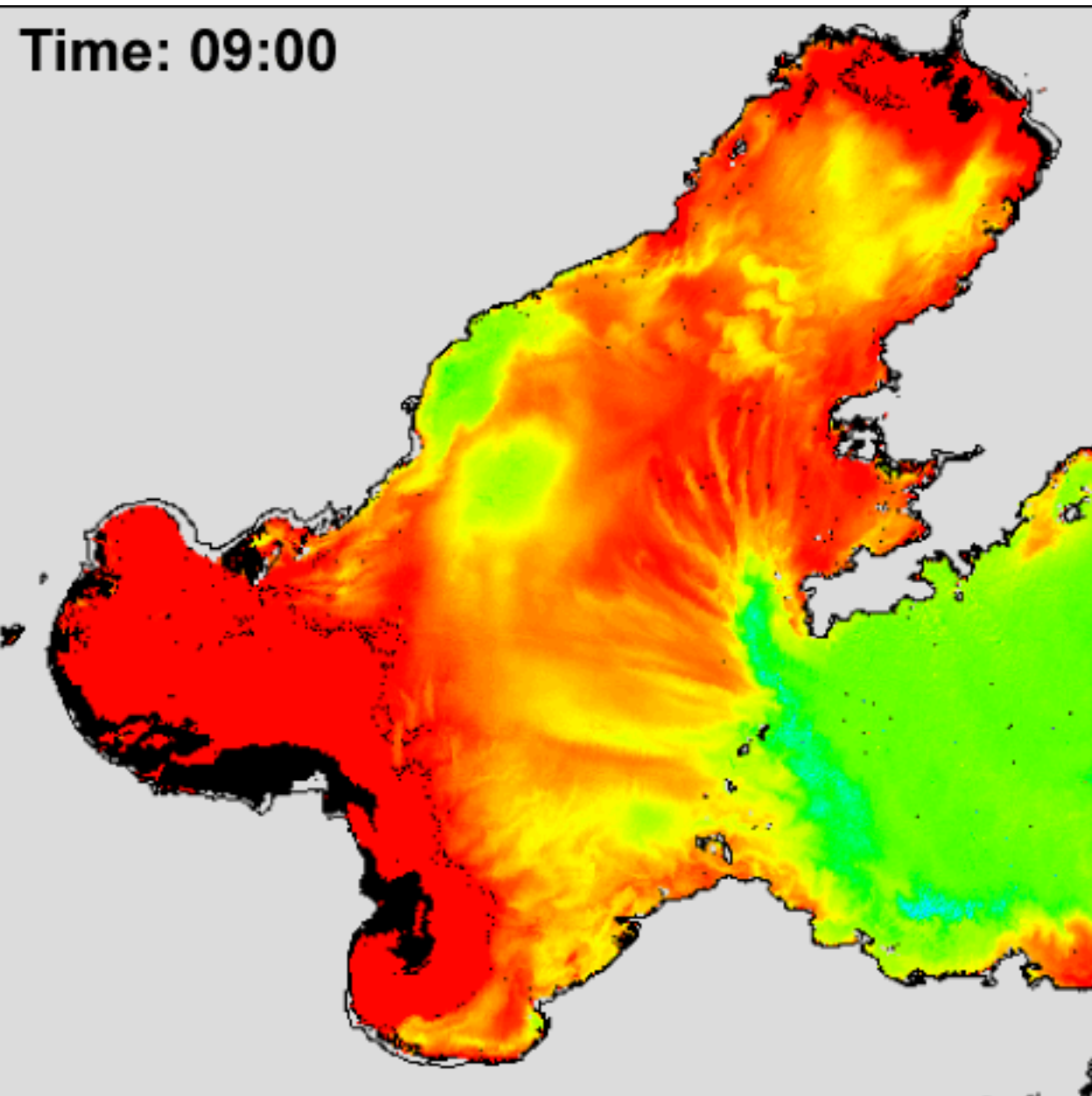
GOCI NOAA-MSL12 $K_d(490)$ (2012-03-25)



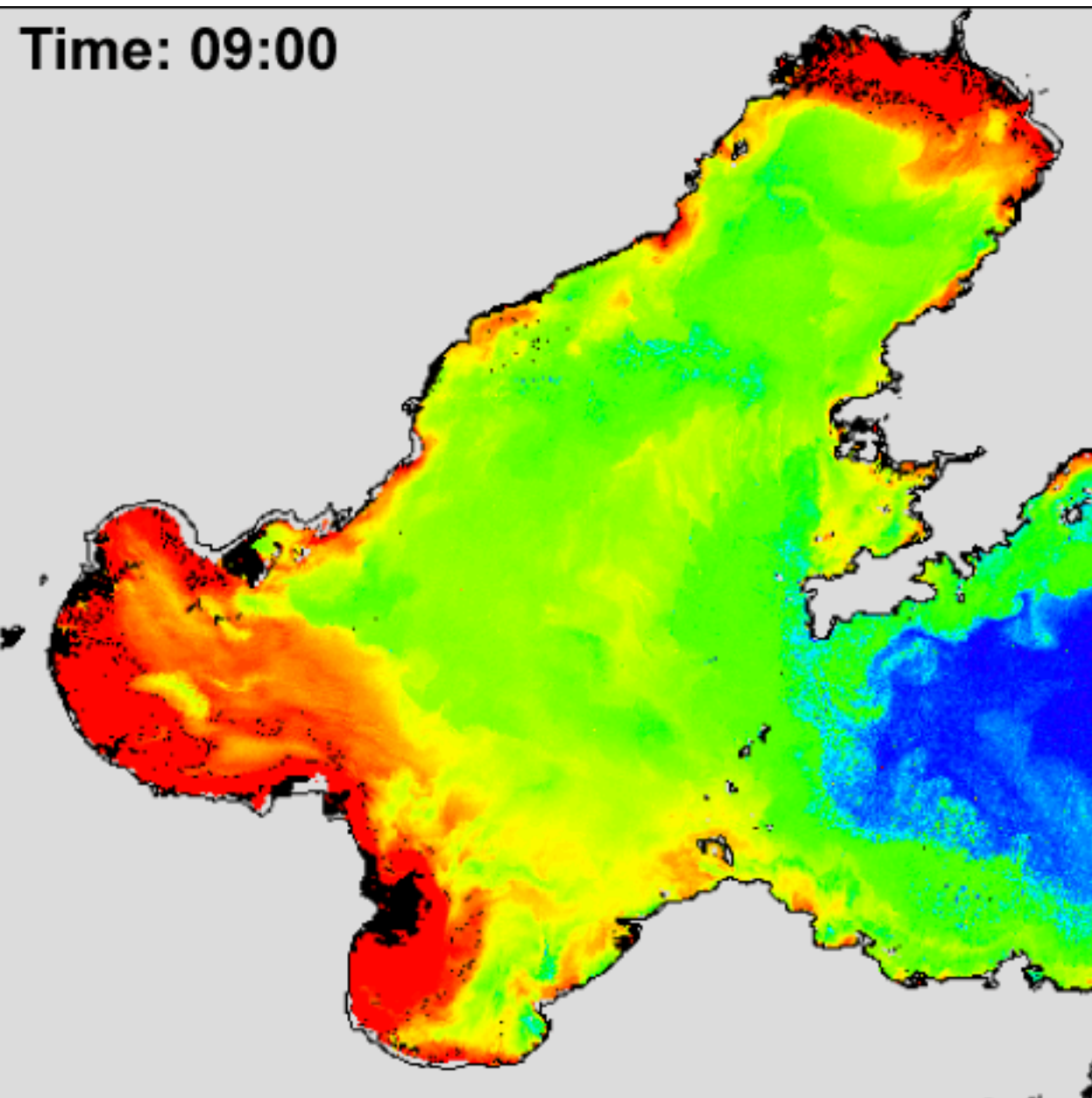
**Diurnal Changes
(Box1)**



GOCI NOAA-MSL12 $K_d(490)$ (2012-03-25)

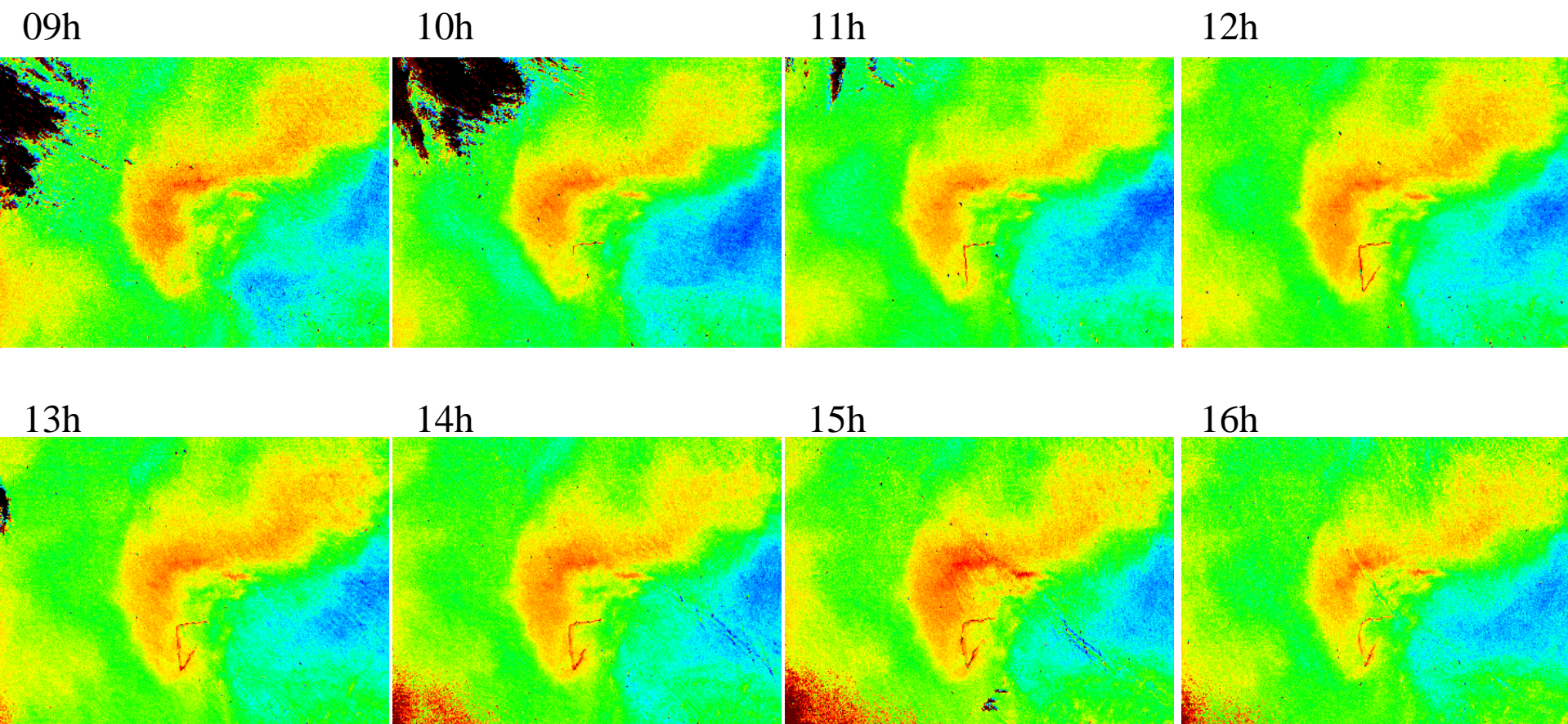


GOCI NOAA-MSL12 $K_d(490)$ (2012-08-23)



**GOCI Images in
Dump Site in the Yellow Sea**

GOCI NOAA-MSL12 **$K_d(490)$** (Jul. 19, 2011)

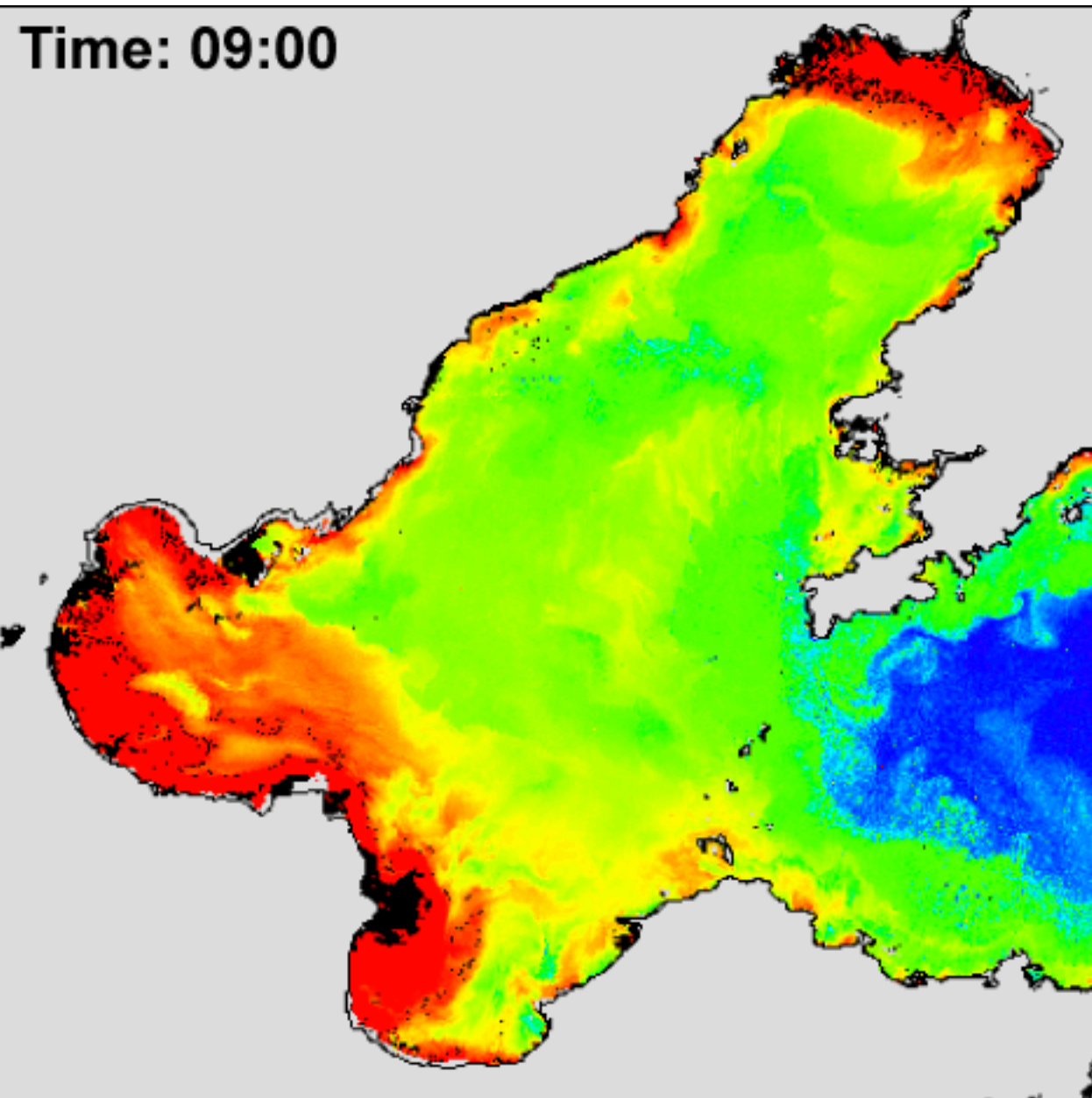


Summary and Conclusions

- The GOCl ocean color products for the GOCl coverage region have been derived using an iterative NIR-corrected atmospheric correction algorithm.
- Validation results show a reasonably good agreement between GOCl retrievals and in situ measurements.
- This study demonstrates that GOCl ocean color products can be confidently used to characterize and quantify the ocean environments as well as the diurnal variability of the marine ecosystem in the western Pacific.
- This unique capability from geostationary satellite sensor can complement the ocean color observations of other polar-orbiting satellites such as MODIS and VIIRS, which have a global coverage but lack the temporal resolution to monitor the dynamics of marine environments on an hourly basis.

Thank you!

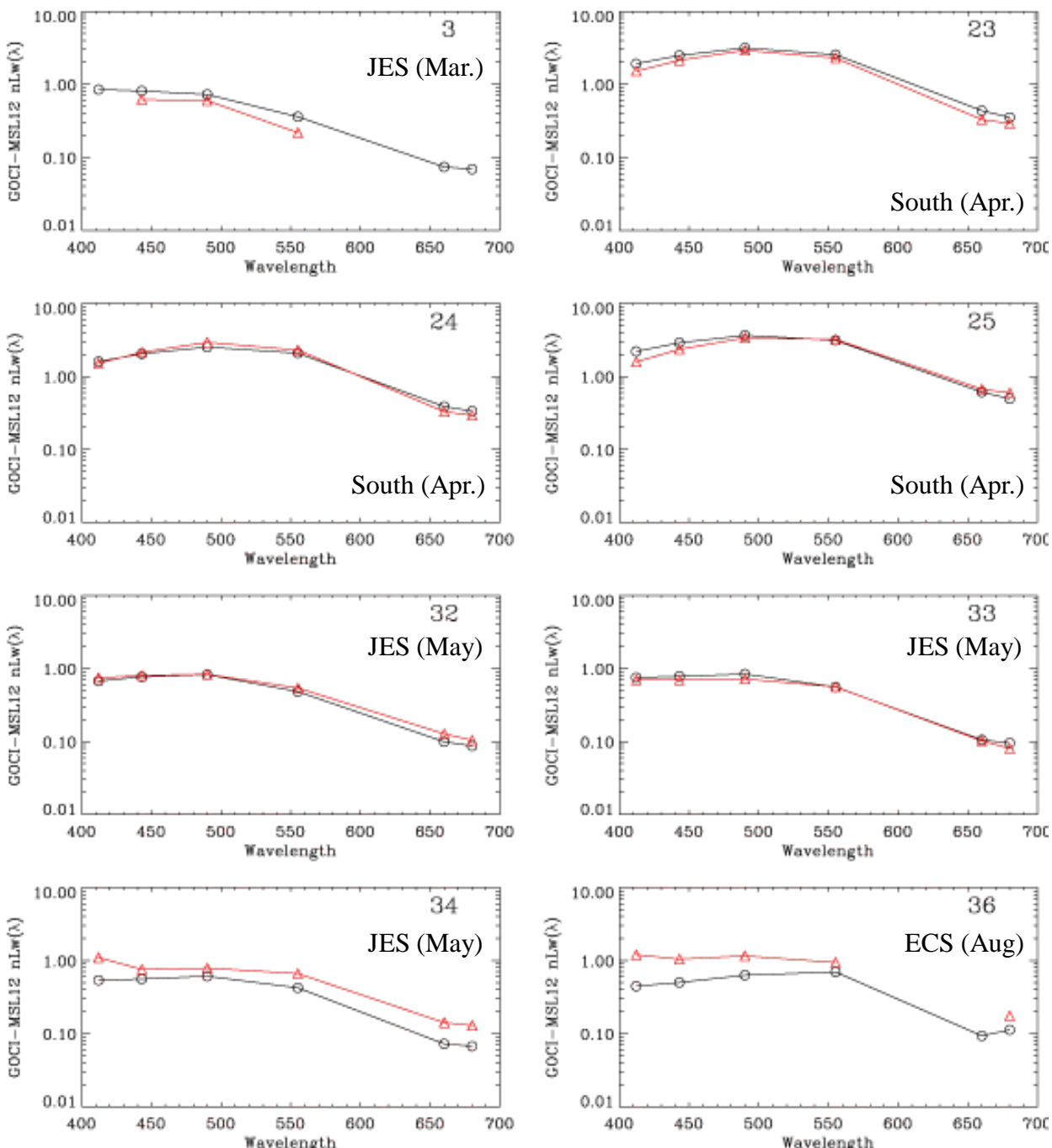
GOCI NOAA-MSL12 $K_d(490)$ (2012-08-23)



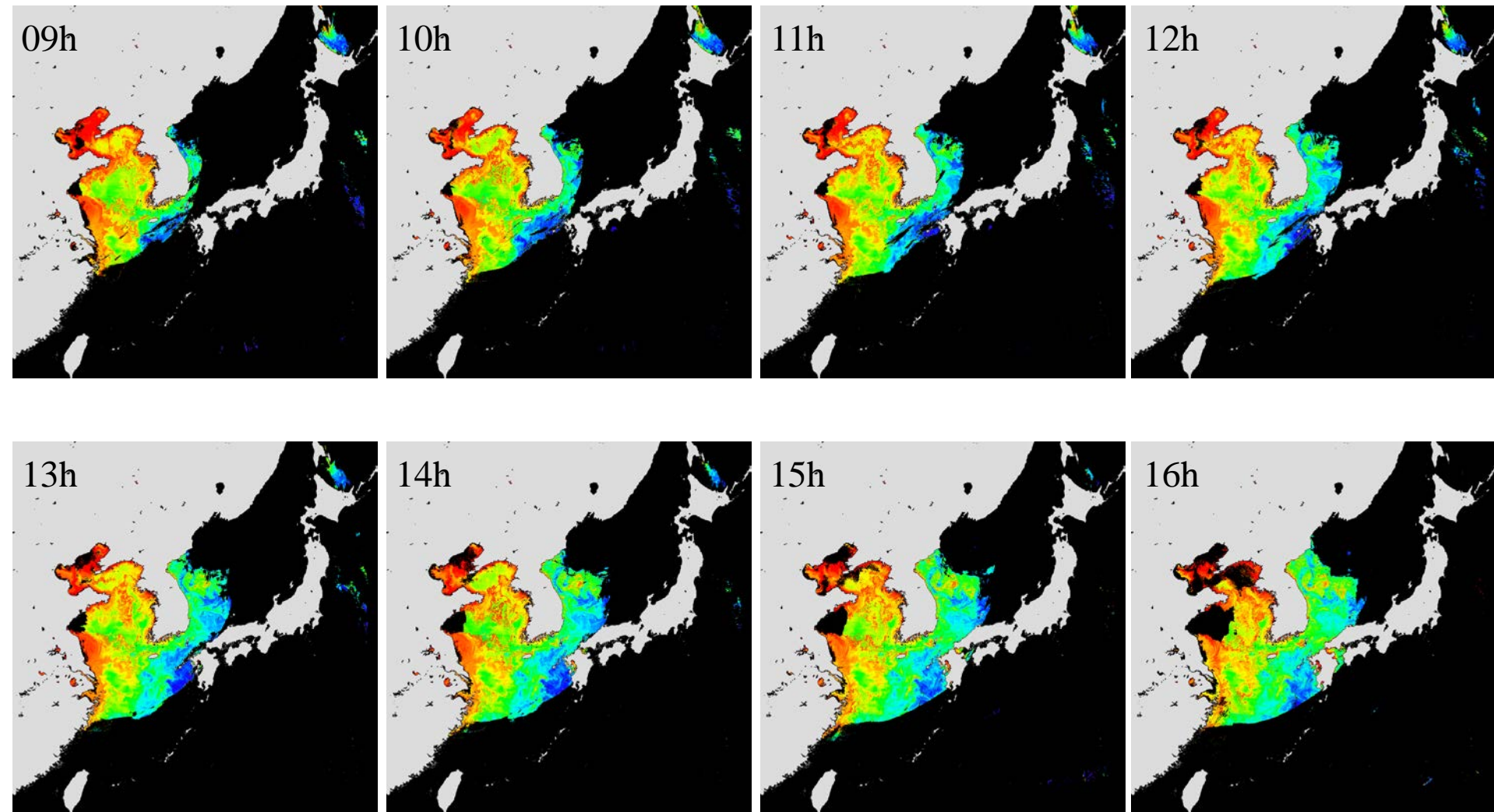
Backup

Black-in situ, red-GOCI

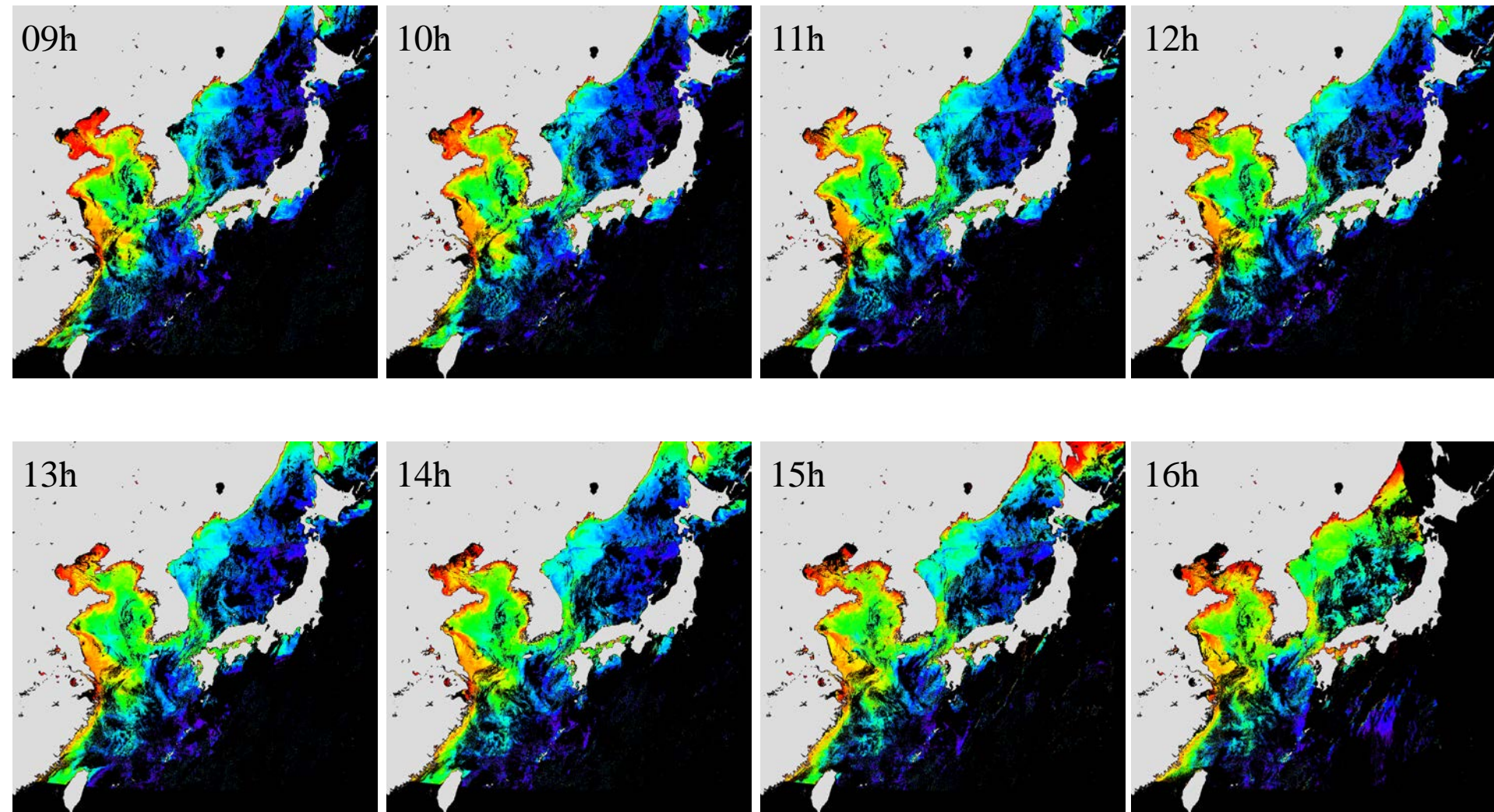
Spectral shape of *in situ* and GOCI-derived $nL_w(\lambda)$ measurements



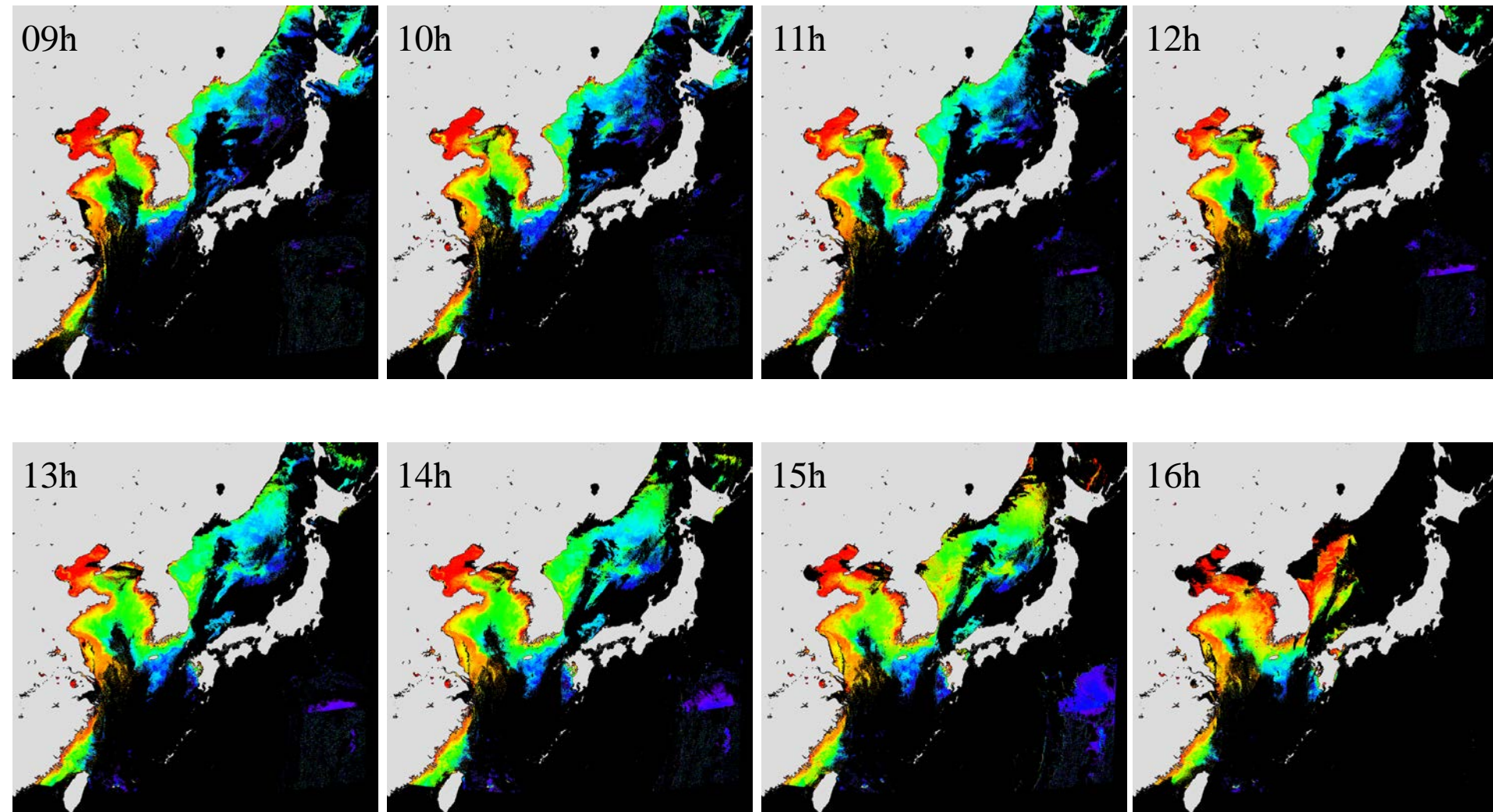
GOCI-MSL12 *Chl-a* (Apr. 26, 2012)



GOCI-MSL12 *Chl-a* (Oct. 2, 2012)

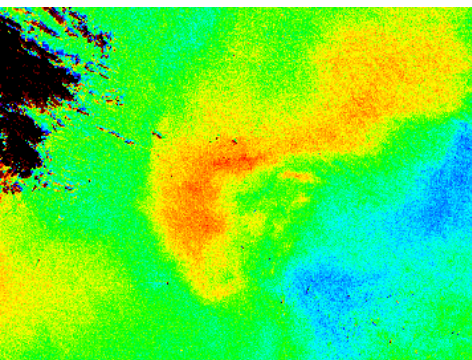


GOCI-MSL12 *Chl-a* (Oct. 18, 2012)

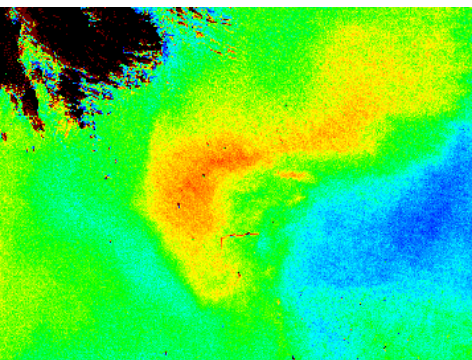


GOCI NOAA-MSL12 *Chl-a* (Jul. 19, 2011)

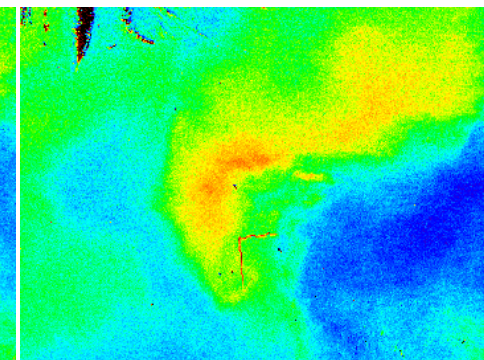
09h



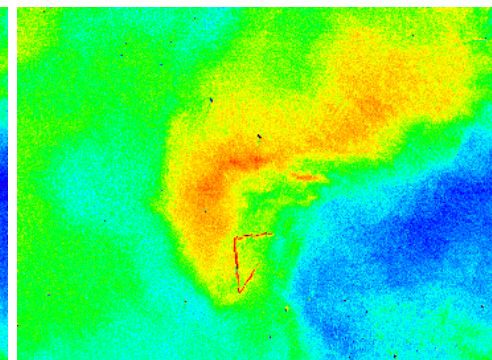
10h



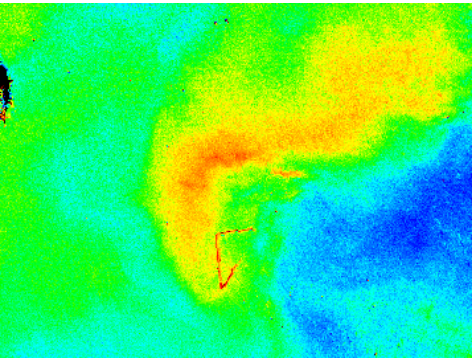
11h



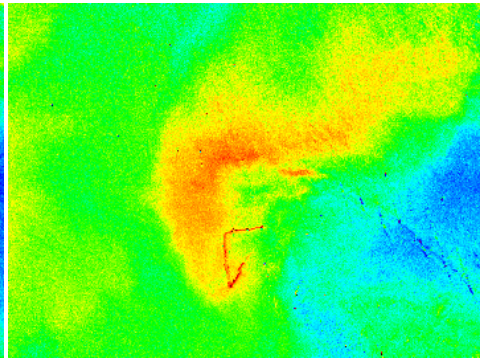
12h



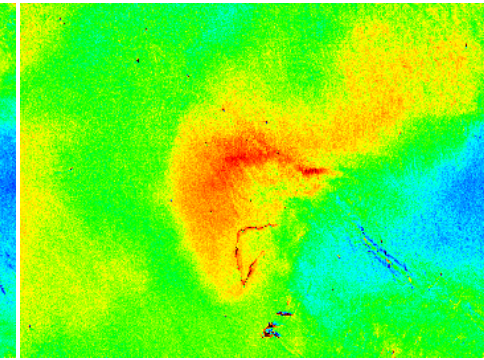
13h



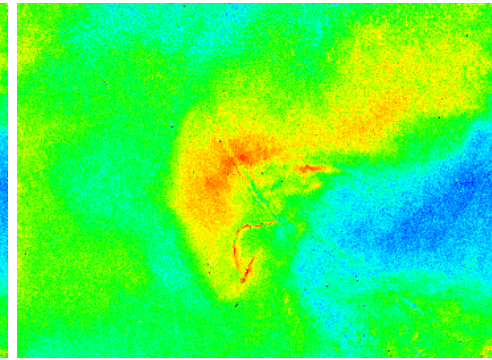
14h



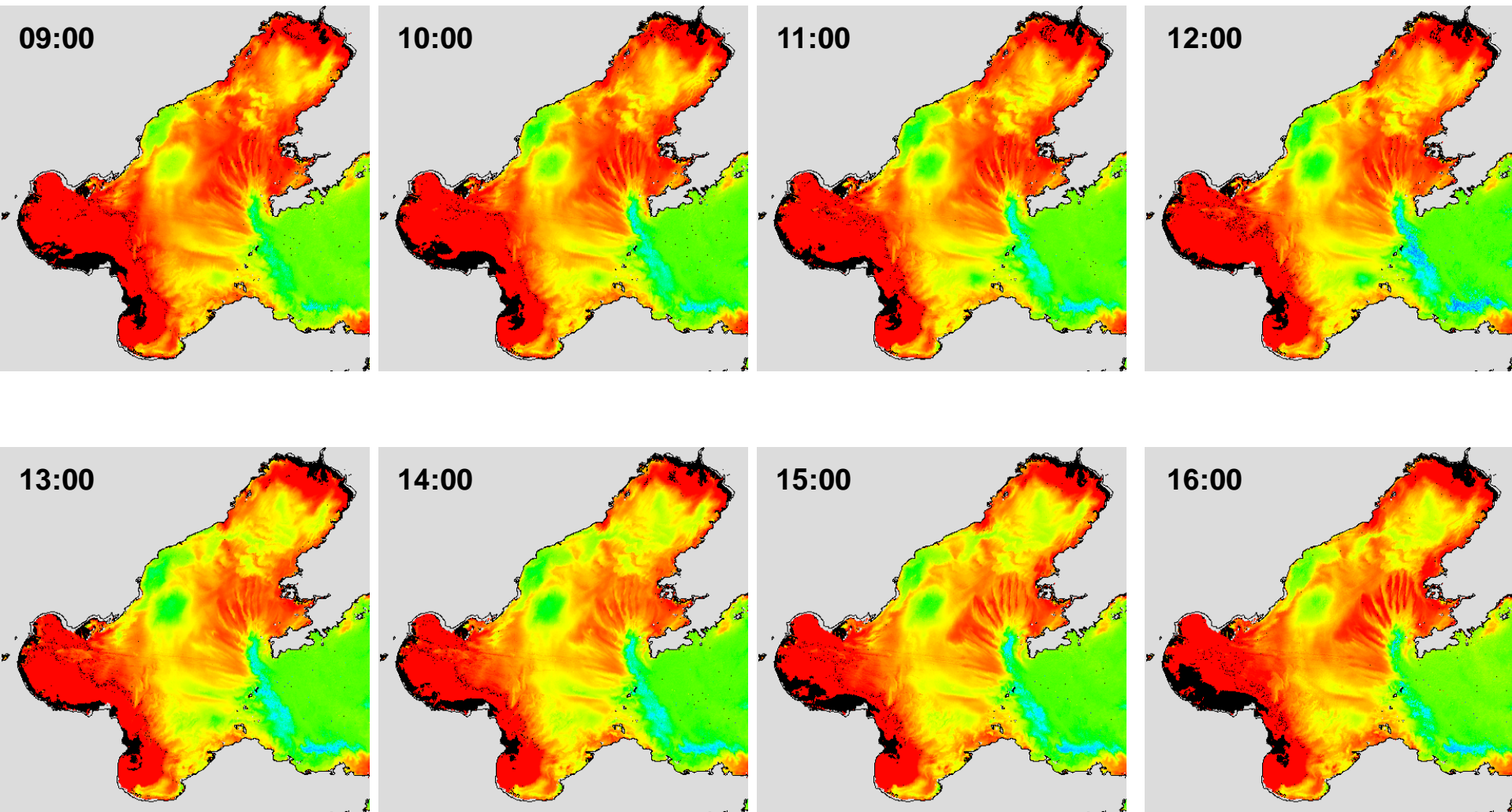
15h



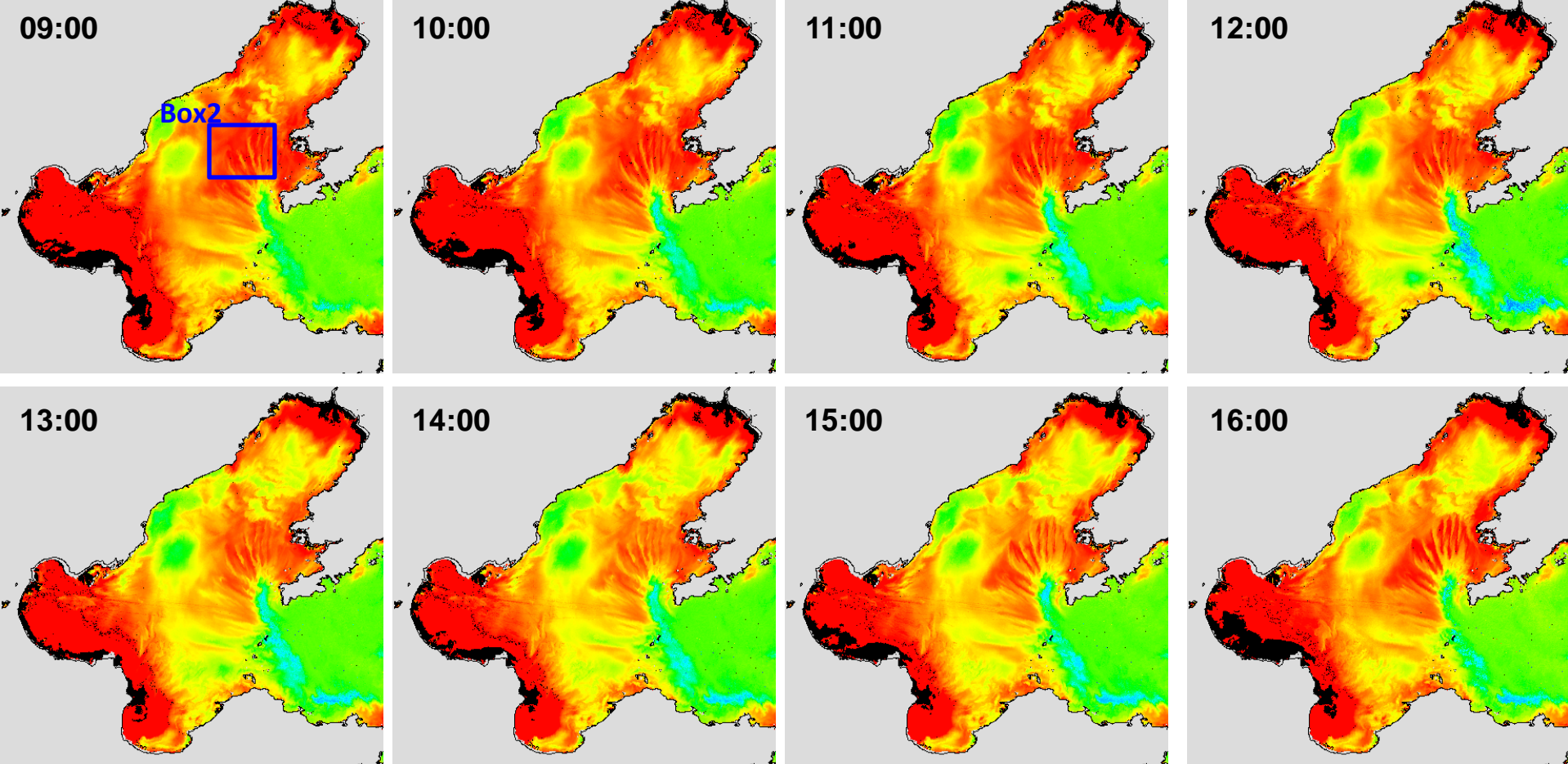
16h



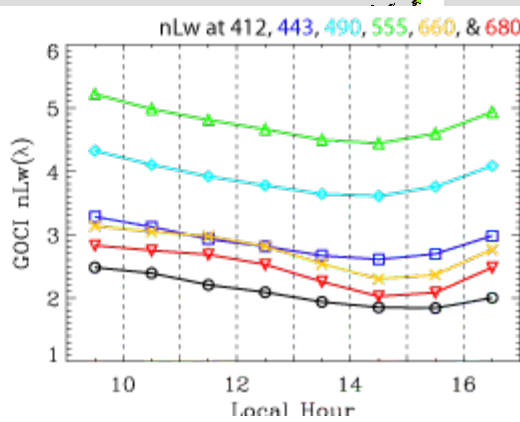
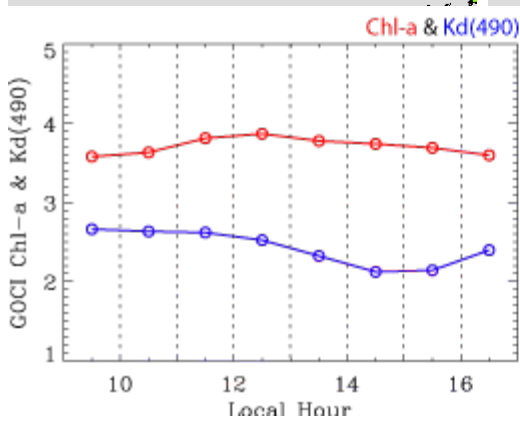
GOCI NOAA-MSL12 K_d (490) (2012-03-25)



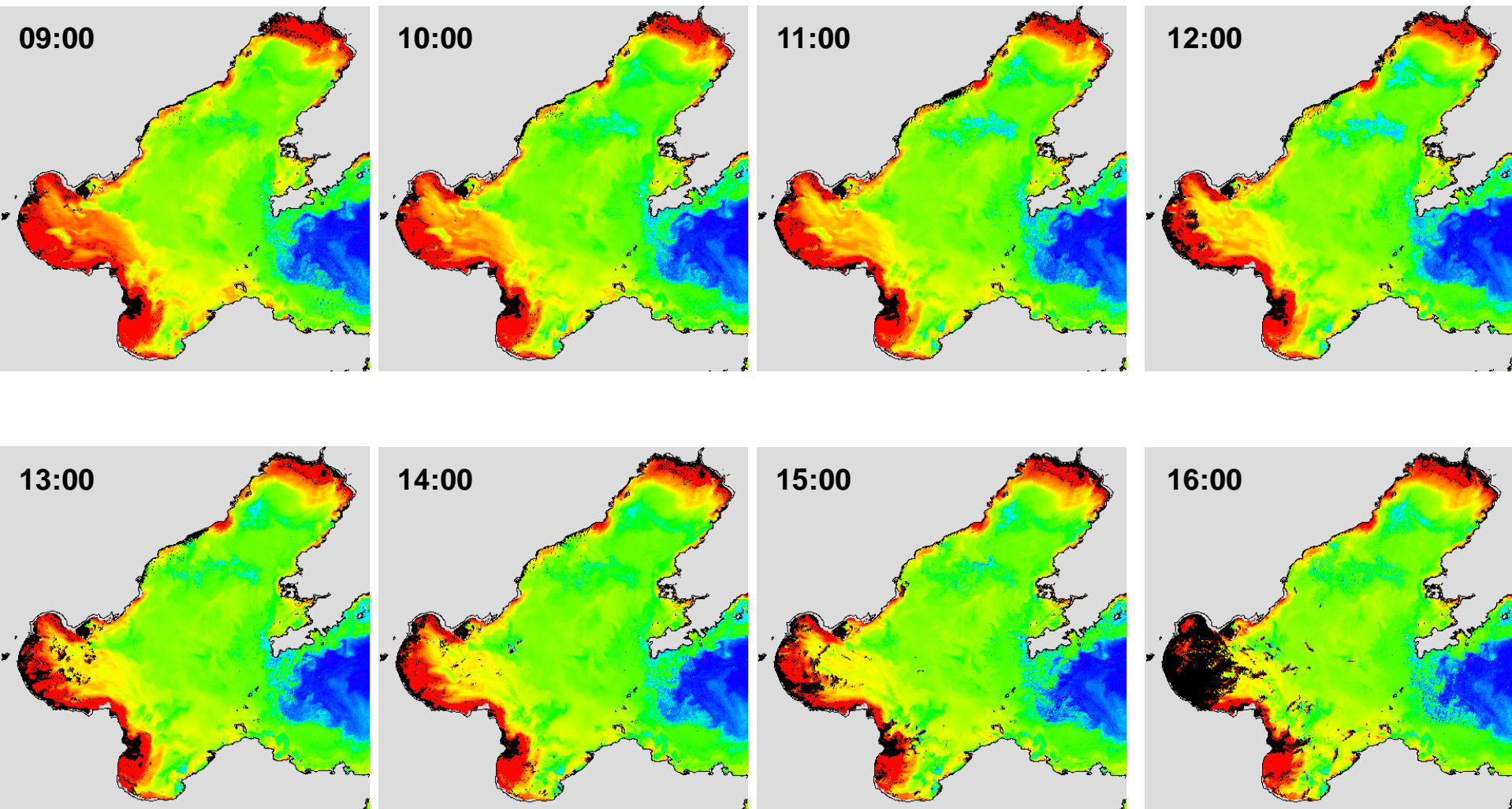
GOCI NOAA-MSL12 $K_d(490)$ (2012-03-25)



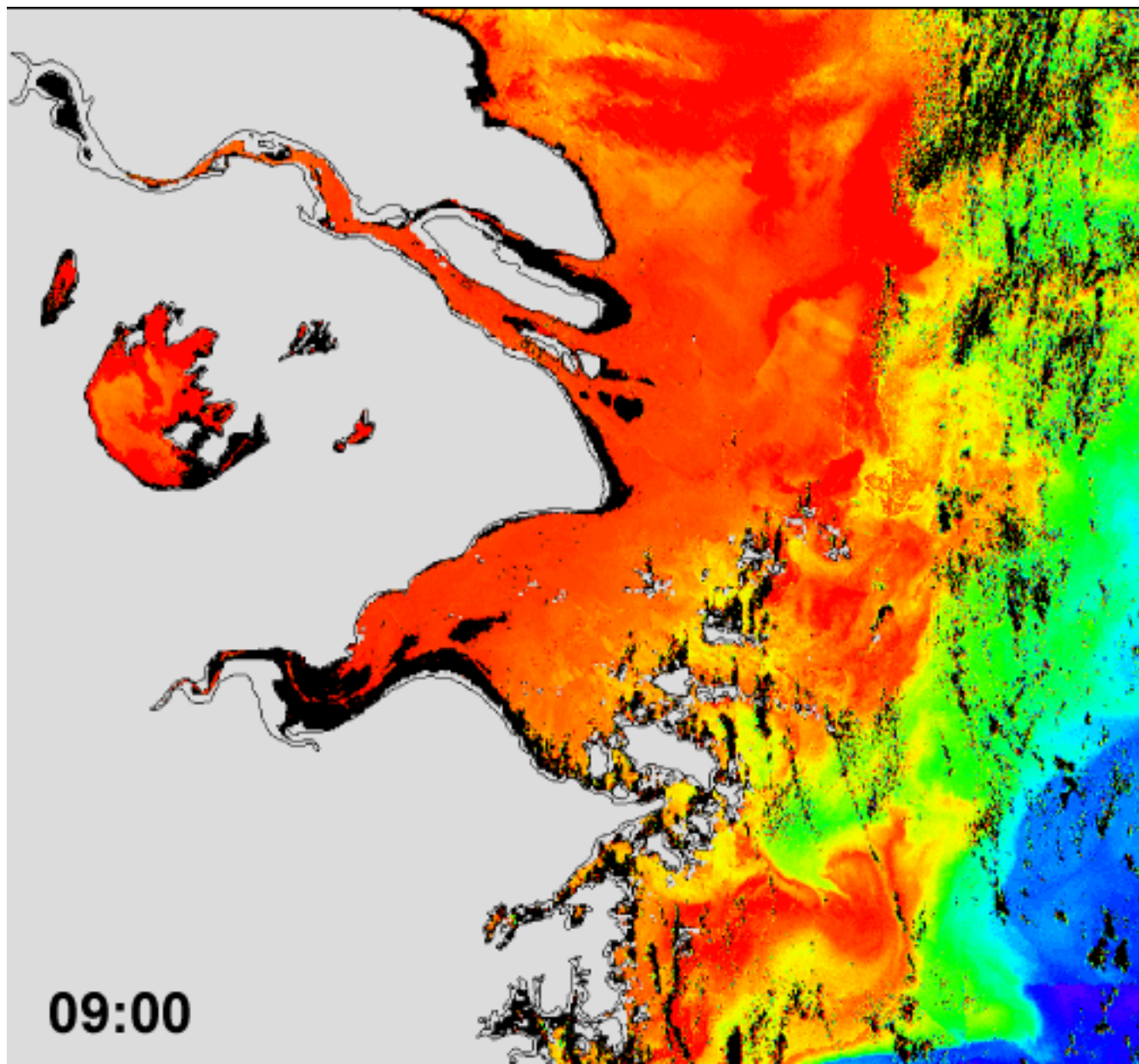
**Diurnal Changes
(Box2)**



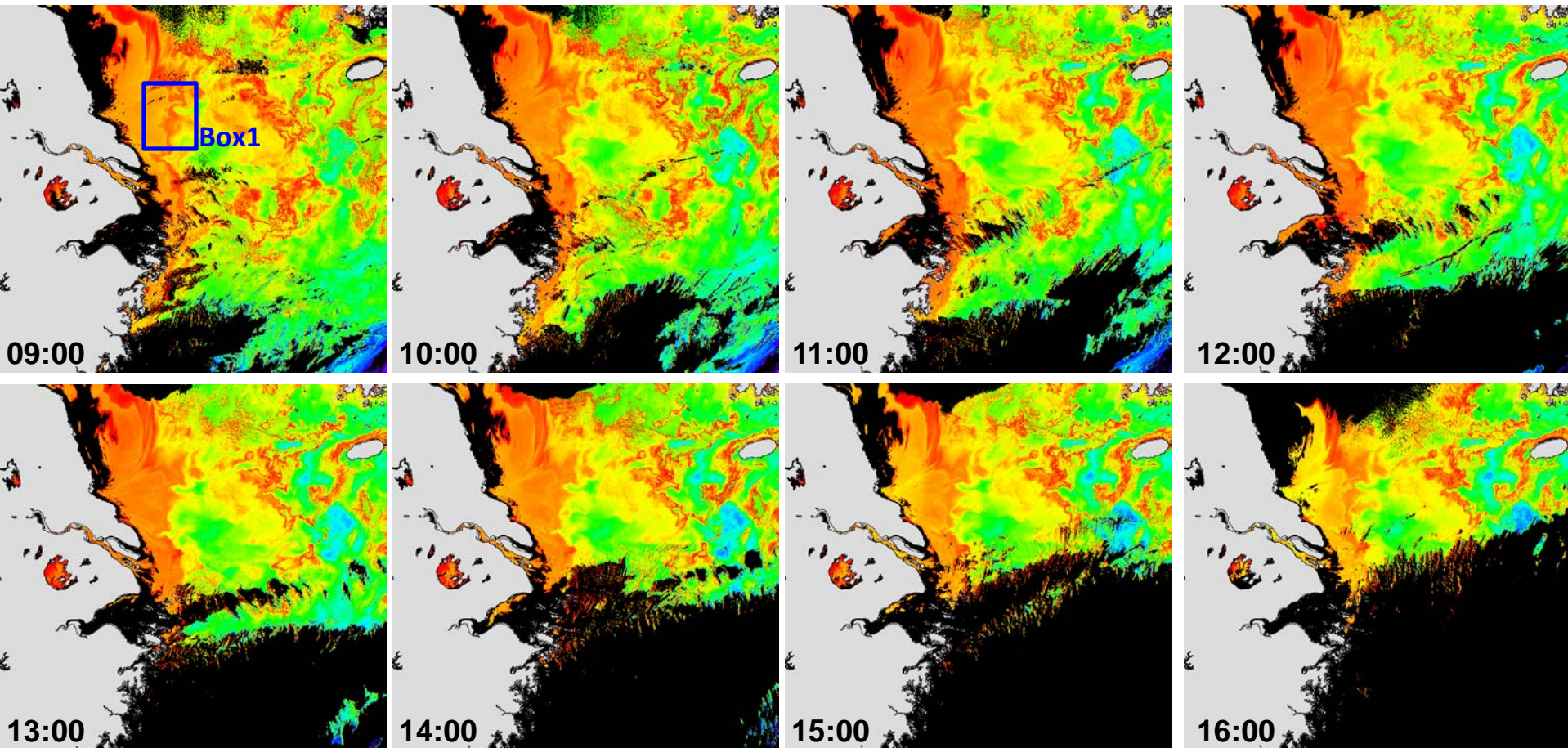
GOCI NOAA-MSL12 K_d (490) (2012-08-23)



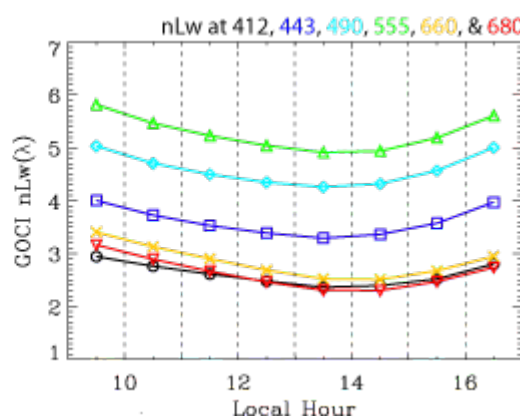
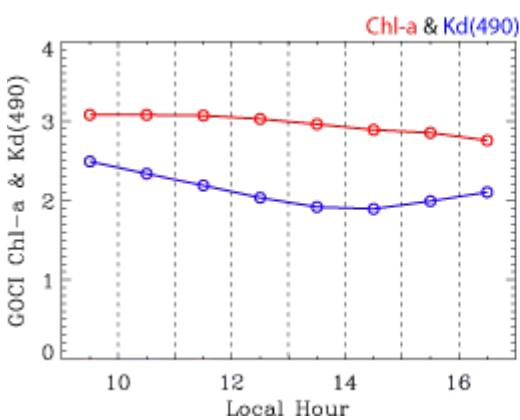
GOCI NOAA-MSL12 Chl-a (2012-07-29)



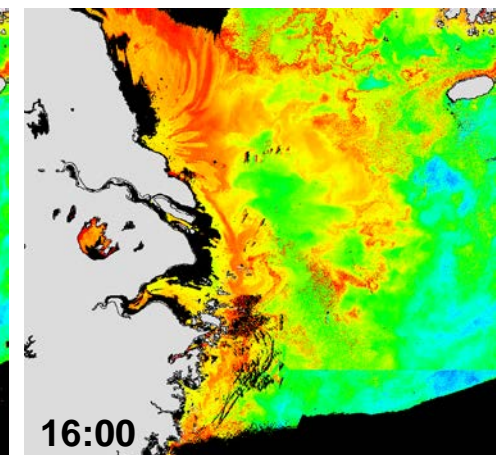
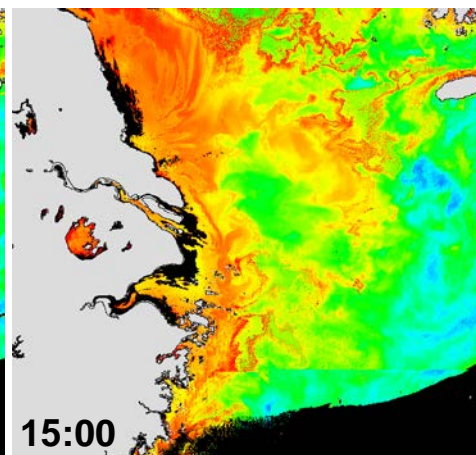
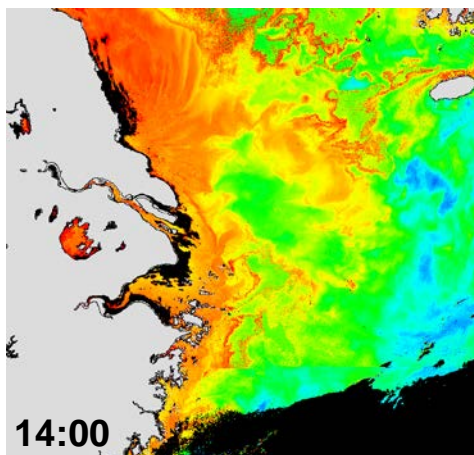
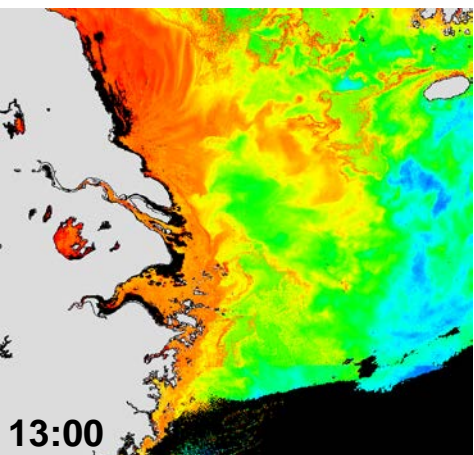
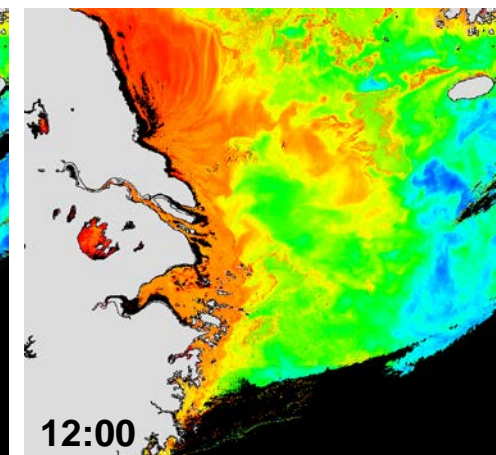
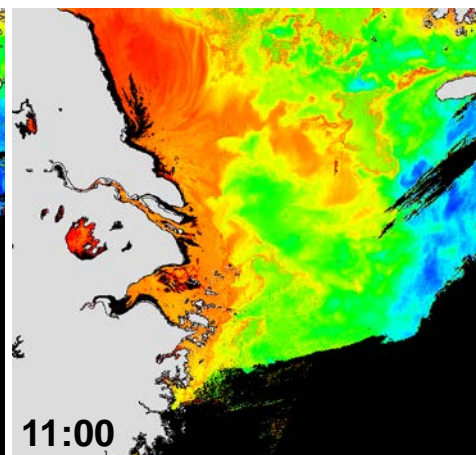
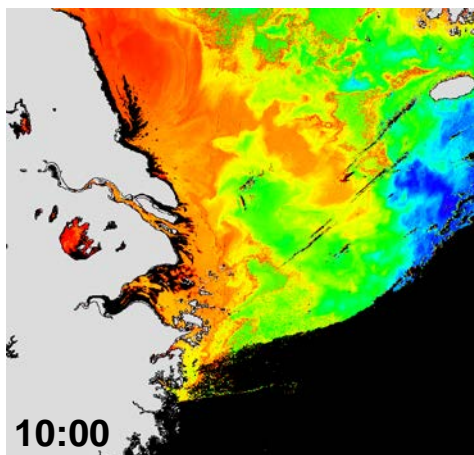
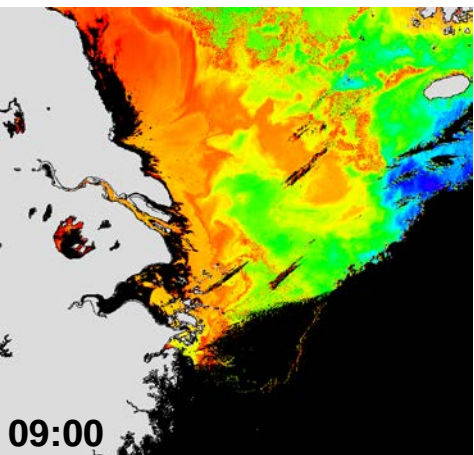
GOCI NOAA-MSL12 Chl-a (2012-04-27)



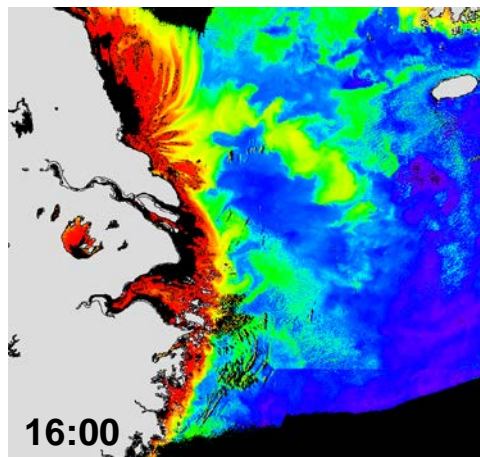
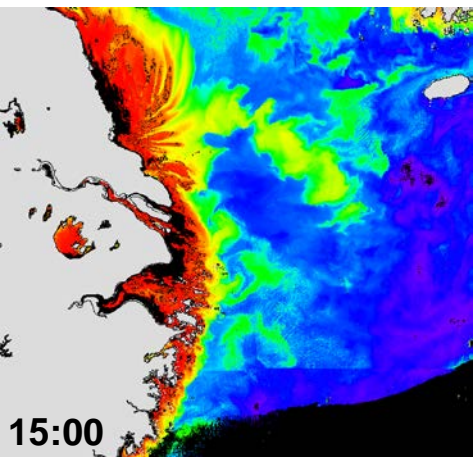
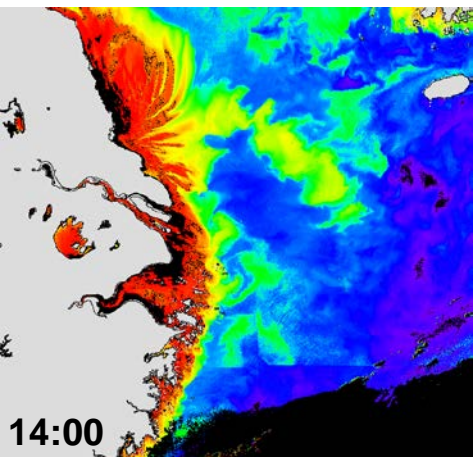
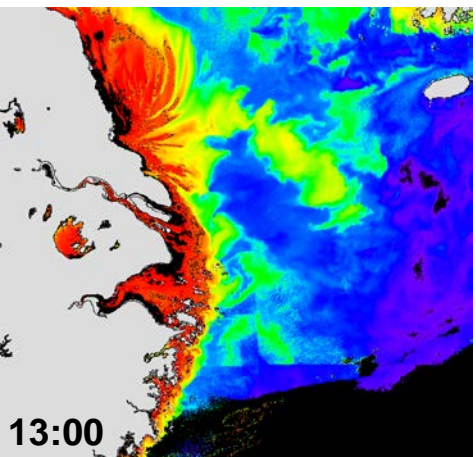
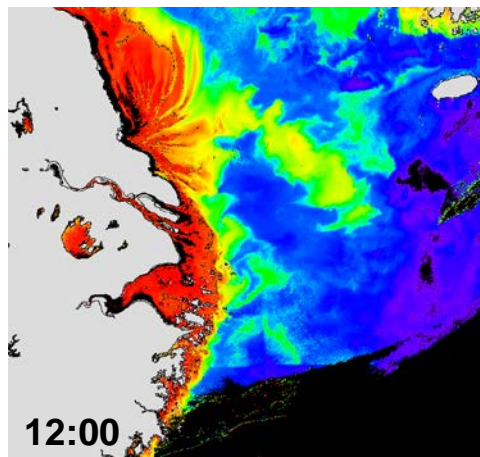
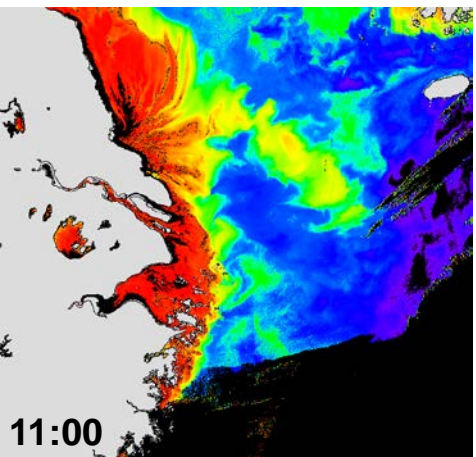
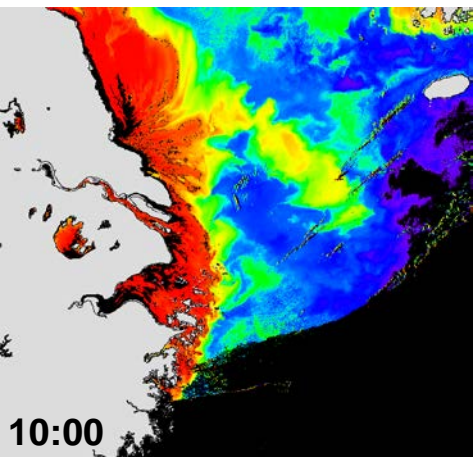
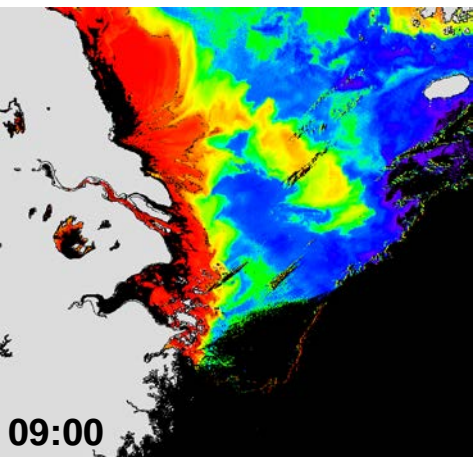
Diurnal Changes



GOCI NOAA-MSL12 Chl-a (2012-04-26)



GOCI NOAA-MSL12 $K_d(490)$ (2012-04-26)



GOCI NOAA-MSL12 Chl-a (2012-04-27)

